Organ dose conversion coefficients for voxel models of the reference male and female from idealized photon exposures

2007 Phys. Med. Biol. 52 2123

(http://iopscience.iop.org/0031-9155/52/8/006)

IOP Publishing Physics in Medicine and Biology

Phys. Med. Biol. **52** (2007) 2123–2145 doi:10.1088/0031-9155/52/8/006

Organ dose conversion coefficients for voxel models of the reference male and female from idealized photon exposures

H Schlattl, M Zankl and N Petoussi-Henss

GSF—National Research Center for Environment and Health, Institute of Radiation Protection, Ingolstädter Landstr. 1, 85764 Neuherberg, Germany

E-mail: helmut.schlattl@gsf.de

Received 20 November 2006, in final form 24 January 2007
Published 27 March 2007
Online at stacks.iop.org/PMB/52/2123

Abstract

A new series of organ equivalent dose conversion coefficients for whole body external photon exposure is presented for a standardized couple of human voxel models, called Rex and Regina. Irradiations from broad parallel beams in antero-posterior, postero-anterior, left- and right-side lateral directions as well as from a 360° rotational source have been performed numerically by the Monte Carlo transport code EGSnrc. Dose conversion coefficients from an isotropically distributed source were computed, too. The voxel models Rex and Regina originating from real patient CT data comply in body and organ dimensions with the currently valid reference values given by the International Commission on Radiological Protection (ICRP) for the average Caucasian man and woman, respectively. While the equivalent dose conversion coefficients of many organs are in quite good agreement with the reference values of ICRP Publication 74, for some organs and certain geometries the discrepancies amount to 30% or more. Differences between the sexes are of the same order with mostly higher dose conversion coefficients in the smaller female model. However, much smaller deviations from the ICRP values are observed for the resulting effective dose conversion coefficients. With the still valid definition for the effective dose (ICRP Publication 60), the greatest change appears in lateral exposures with a decrease in the new models of at most 9%. However, when the modified definition of the effective dose as suggested by an ICRP draft is applied, the largest deviation from the current reference values is obtained in postero-anterior geometry with a reduction of the effective dose conversion coefficient by at most 12%.

1. Introduction

Ionizing radiation is a natural phenomenon the human body has to cope with. Additionally, it can be exposed to artificially created radiation in the occupational or a medical environment. Important quantities in radiation protection to value the radiation received from external sources are organ dose conversion coefficients that relate organ doses to measurable physical quantities. From the organ doses the 'effective dose' can be calculated, which takes into account the radiation sensitivity of the individual organs by different tissue weighting factors (ICRP 1991).

Since *in vivo* measurements of organ doses are not possible, the conversion coefficients have to be determined numerically. An important part in these computations are virtual models of the human anatomy, which have been evolved in the last few decades starting from simple spheres over mathematical models to modern CT (computed tomography) or MRI (magnetic resonance imaging) based models.

The still valid standard values for radiation protection provided by the International Commission on Radiological Protection (ICRP 1996) have been calculated by mathematical phantoms, where the body and the organs are composed by geometrical shapes (Snyder *et al* 1978, Kramer *et al* 1982). This phantom type is sometimes called 'MIRD-type' due to having been introduced in Pamphlet no. 5 of the Medical Internal Radiation Dose Committee (MIRD).

Various groups have already developed voxel models based on CT or MRI images of individual phantoms (Gibbs *et al* 1984, Zankl *et al* 1988, Zubal *et al* 1994, Xu *et al* 2000, Zankl and Wittmann 2001, Petoussi-Henss *et al* 2002). However, being derived from individual patient data, the models do not represent the average Caucasian man or woman as defined by ICRP Publications 23 (ICRP 1975) or 89 (ICRP 2002). A first step in this direction was performed by Dimbylow (1996), who adjusted a segmented MRI whole-body data set to yield a phantom (NORMAN) with body mass and height as well as organ masses in agreement with the reference data from ICRP 23. Recently, more efforts have been made to build human models, e.g., Godwin and Klara (Zankl *et al* 2005), and MAX06 and FAX06 (Kramer *et al* 2006), where also the individual organ masses and densities conform to the values of ICRP Publications 70 (ICRP 1995) and 89 (ICRP 2002).

In the present work, organ dose conversion coefficients are presented for idealized external photon exposure, obtained with newly developed models named 'Rex' and 'Regina'. Rex and Regina are improved versions of Godwin and Klara and, in addition to the standard organs, they contain, e.g., also lymphatic nodes and oral mucosa which are part of the remainder tissue as proposed in ICRP draft recommendations (ICRP 2006). Furthermore, their skeletons comply with ICRP Publications 70 (ICRP 1995) and 89 (ICRP 2002). Rex and Regina were developed in close cooperation with and supervision by the ICRP in order to cover several features important to external and internal dosimetry. They will be used as the standard human models for the computation of dose conversion coefficients in occupational protection as well as for the protection of the patient and the general public (ICRP 2006).

The equivalent dose conversion coefficients have been computed by the Monte Carlo method, where the particle transport has been performed by EGSnrc (Kawrakow and Rogers 2003). To decrease the statistical uncertainty in rather small organs, importance sampling has been implemented into the user code. By this method, the number of particles is enhanced in small predefined regions while simultaneously reducing the contribution (weight) of those particles to the total flux appropriately.

In the next section, a brief description of our virtual human models will be provided, followed by details about the dosimetry of the bones (section 2.2) and the computational

method (section 2.3). After presenting the results for external photon sources in standard idealized geometries (section 3), the implied changes compared to the current reference equivalent dose conversion coefficients of ICRP Publication 74 (ICRP 1996) will be discussed.

2. Computational models

2.1. The voxel models

At GSF, several adult voxel models have been developed until now (Zankl and Wittmann 2001, Petoussi-Henss *et al* 2002, Zankl *et al* 2005). From this database the models Golem (height 176 cm, weight 60 kg) and Laura (167 cm, 59 kg) have been chosen as the bases of those voxel models, which should represent the male and female adult ICRP Reference person. Initially, the voxel heights of Golem and Laura have been adjusted to yield a phantom height in agreement with ICRP Publication 89 (ICRP 2002), i.e., 176 and 163 cm, respectively. The in-plane voxel size was then scaled to obtain the same skeleton volumes as given by ICRP 70 (ICRP 1995) and 89 (ICRP 2002). These requirements led to voxel dimensions of $2.137 \times 2.137 \times 8.0\ \mathrm{mm}^3$ for the male and $1.775 \times 1.775 \times 4.84\ \mathrm{mm}^3$ for the female model. The ensuing steps consisted of the adjustment of the individual organ dimensions to the requirements of ICRP Publication 89 and the inclusion of additional organs, like lymphatic nodes, which were not discernable in the original CT data. The locations of the latter were defined by consulting anatomical books. For all modification steps, the software 'VolumeChange' was applied, which has been developed at GSF (Becker *et al* 2007). The resulting voxel models, Rex and Regina, will be adopted by the ICRP as computational models representing the Reference Male and Female in the near future.

The skeleton has been sub-segmented into 19 bones and bone groups, and each of these into cortical bone, spongiosa and—where appropriate—medullary cavities. The individual bone components (mineral bone, cartilage, active and inactive bone marrow, and miscellaneous tissue) have been distributed appropriately and their masses and volumes agree with data of ICRP Publications 70 (ICRP 1995) and 89 (ICRP 2002). A more detailed description is available elsewhere (Zankl *et al* 2007). A list of tissues and their elemental compositions used for Regina is provided in table 1. Apart from soft and spongiosa tissues their compositions are taken directly from ICRP (2002). For Regina and Rex four types of soft tissues are used instead of only one as in the previous models; these have been evaluated by averaging the compositions of organs with similar consistence (see the footnote of table 1). By the introduction of four instead of one soft-tissue type, the exact mass energy-absorption coefficients of each organ (ICRP 2002) could be reproduced with an accuracy of 4% for all organs. With one soft tissue the discrepancies to the exact mass energy-absorption coefficients could amount to 10% or more.

All tissues are common to both phantoms, except the various spongiosa types. The red bone marrow content and the ratio of red and yellow bone marrow differ from bone to bone (ICRP 1995). Hence, the relative amounts of the bone components vary among the different bone groups, resulting in bone-specific spongiosa compositions. Since parts of inactive bone marrow (in the medullary cavities), cartilage and mineral bone have been segmented explicitly, and their volumes are not the same in Regina and Rex, the spongiosa compositions slightly differ in the male and female model (Zankl *et al* 2007).

2.2. Dosimetric treatment of bones

Since the exact structure of spongy cancellous bone is too fine to be resolved by conventional CT scanners, the direct association of each voxel with a single bone component is hardly

Table 1. Elemental composition (in mass per cent) of the tissues assigned to Regina, the voxel model representing the ICRP Reference Female. In the last column, the mass densities, based on ICRU Report 46 (ICRP 1992), are provided in g cm^{-3}. The spongiosa (SP) tissues have been derived from a mixture of all bone components (see the text), and below the half of femur or humerus no active bone marrow (RBM) is present in the extremities.

Tissue	H	C	N	O	Na	Mg	P	S	Cl	K	Ca	Fe	Dens.
Teeth	2.2	9.5	2.9	42.1		0.7	13.7				28.9		2.75
Mineral bone	3.5	16.0	4.2	44.5	0.3	0.2	9.5	0.3			21.5		1.92
SP (no RBM)	9.5	47.5	1.7	33.4	0.17	0.05	2.4	0.21	0.03	0.01	4.95		1.12
SP upper humeri	8.6	37.7	2.5	40.7	0.20	0.10	3.2	0.27	0.04	0.01	6.61	0.018	1.18
SP clavicles	8.5	37.2	2.6	41.0	0.20	0.10	3.3	0.27	0.04	0.01	6.80	0.018	1.19
SP cranium	8.0	32.5	2.8	43.7	0.22	0.11	4.0	0.30	0.05	0.02	8.27	0.016	1.25
SP upper femora	10.4	51.3	1.8	32.9	0.13	0.07	1.1	0.17	0.01	0.004	2.03	0.027	1.05
SP mandible	8.6	36.9	2.6	41.4	0.20	0.10	3.3	0.27	0.04	0.01	6.68	0.021	1.19
SP pelvis	9.5	42.6	2.5	38.8	0.16	0.11	2.0	0.23	0.02	0.01	4.00	0.035	1.11
SP ribs	9.7	41.2	2.8	41.0	0.15	0.14	1.6	0.22	0.02	0.01	3.02	0.056	1.09
SP scapulae	9.3	42.2	2.4	38.5	0.17	0.10	2.4	0.23	0.03	0.01	4.78	0.026	1.13
SP cervical spine	9.1	37.8	2.9	42.7	0.17	0.14	2.3	0.25	0.03	0.01	4.57	0.048	1.14
SP thoracic sp.	9.8	41.9	2.8	40.7	0.14	0.14	1.4	0.22	0.02	0.01	2.74	0.057	1.08
SP lumbar spine	8.7	35.1	3.0	43.9	0.19	0.14	2.8	0.27	0.04	0.01	5.74	0.042	1.17
SP sacrum	10.2	44.6	2.7	39.5	0.12	0.14	0.9	0.20	0.01	0.003	1.52	0.063	1.05
SP sternum	9.9	42.6	2.8	40.4	0.14	0.14	1.3	0.21	0.02	0.005	2.44	0.059	1.08
RBM	11.5	64.4	0.7	23.1	0.1		0.1	0.1					0.98
Cartilage	9.6	9.9	2.2	74.4	0.5		2.2	0.9	0.3				1.10
Skin	10.0	20.4	4.2	64.5	0.2		0.1	0.2	0.3	0.1			1.09
Blood	10.2	11.0	3.3	74.5	0.1		0.1	0.2	0.3	0.2		0.1	1.06
Muscle tissue	10.2	14.3	3.4	71.0	0.1		0.2	0.3	0.1	0.4			1.05
Soft tissue 1[a]	10.5	13.9	2.7	71.8	0.17		0.27	0.17	0.23	0.27	0.03		1.05
Soft tissue 2[b]	10.2	18.3	3.6	67.0	0.17		0.17	0.23	0.17	0.17			1.05
Soft tissue 3[c]	10.5	10.8	2.4	75.4	0.15		0.15	0.15	0.21	0.18			1.04
Soft tissue 4[d]	10.5	26.2	2.7	59.7	0.10		0.20	0.29	0.19	0.20			1.03
Lymph	10.8	4.1	1.1	83.2	0.3			0.1	0.4				1.03
Mammary gland	10.6	33.2	3.0	52.7	0.1		0.1	0.2	0.1				1.02
Adipose tissue	11.4	59.8	0.7	27.8	0.1		0.1	0.1					0.95
Lung tissue	10.3	10.5	3.1	74.9	0.2		0.2	0.3	0.3	0.2			0.38

[a] Brain, heart, kidney.
[b] Eyes, liver, pancreas.
[c] Stomach, intestine, ovaries, spleen, testes, thyroid, urinary bladder; contains also 0.013% iodine.
[d] Adrenals, gall bladder, oesophagus, pituitary gland, prostate, thymus, tonsils, trachea, ureters, uterus.

possible. Only a few voxels in the shafts of the long bones can be directly identified as bone marrow when segmenting the CT data. For the other voxels, mixture media are to be defined (see table 1).

A direct determination of dose conversion coefficients for active (or red) bone marrow (RBM) can hence not be made as for other organs, to which whole voxels can be uniquely assigned. Therefore, the method described by Zankl *et al* (2002) is employed: the physical transport property of a bone voxel is determined by the mixture medium, from which the total energy deposited in that voxel can be deduced (usually through a Monte Carlo transport code). This amount of energy is then partitioned to the individual bone components according to their mass proportions and mass energy-absorption coefficients. For active bone marrow an additional correction factor is applied which accounts for the extra photo-electrons produced in the bone trabeculae that enter the marrow cavities (King and Spiers 1985). This factor differs between the various bone groups.

Zankl *et al* (2002) originally determined the mass proportions of the bone components directly from the CT data by assuming a linear relation between grey value and marrow content. The volume ratio of active to inactive (or yellow) bone marrow (YBM) was set to a constant value. One disadvantage of this method is that the RBM content (and the contents of other bone components) solely depends on the CT grey values of an individual patient and in most cases therefore does not comply with the average data of ICRP Publications 70 (ICRP 1995) and 89 (ICRP 2002). Moreover, the different cellularity factors, i.e., the ratio of active to total bone marrow, of the bone groups have not been considered correctly. Furthermore, the grey value of a voxel at the outer edge of a bone is often the result of the voxel covering cortical bone and some soft tissue like muscle or adipose tissue ('partial volume effect'). This would be interpreted in the CT method as a mixture of mineral bone and bone marrow. Thus, portions of the bone marrow would be located outside the cortical bone enclosure; this leads to an overestimation of the RBM dose for low photon energies.

In order to overcome these problems, a different strategy has been pursued for Rex and Regina. There, the cortical bone has been segmented explicitly, if possible, and the spongiosa in each bone group has a homogenous composition, but with a different YBM and RBM content in agreement with ICRP Publications 70 (ICRP 1995) and 89 (ICRP 2002). We verified that for external exposures the resulting RBM dose conversion coefficients of this method do not differ much from those of the original CT method. For this purpose, three different versions of bone-marrow distribution have been implemented within one voxel model, and the resulting RBM dose conversion coefficients have been compared. Since, after all modifications performed in Rex and Regina, the original bone CT data do not fit exactly to the segmented bones, none of these models could be employed. However, for a preliminary version of Rex, called Godwin (Zankl *et al* 2005), matching bone CT data are still available.

The first bone-marrow distribution implemented in Godwin (CT) being based on the CT values corresponds to the original method of Zankl *et al* (2002). The ratio of inactive to active bone marrow was chosen such that the total active bone marrow mass agrees in all implementations. CT reflects the case with heterogeneous bone composition; from this version the second bone-marrow distribution was derived by distributing the different bone components in each individual bone uniformly. This implementation, denoted by HOM, thus still has an RBM content in each bone based on the CT data set. In figure 1 it can be seen that the difference between CT and HOM for the resulting dose conversion coefficients of the RBM are hardly visible. Thus, for external photon exposure it is rather irrelevant whether the composition in the bone groups is heterogeneous or homogenous. The third version (CEL) uses also homogenous bone groups like HOM, but the relative RBM and YBM content in each bone group is in agreement with the values of ICRP (1995, 2002). The difference in the RBM dose conversion coefficients of CEL to those of HOM and CT are small but noticeable (figure 1). We therefore conclude that for external exposures the distribution of active bone marrow among the different bone groups has a higher influence on the dose conversion coefficients of the active bone marrow than the spatial distribution of the bone marrow within the bones. Hence, version CEL has been employed in Rex and Regina.

2.3. The Monte Carlo code

The dose conversion coefficients have been computed with a program (user code[1]) developed at GSF, which uses EGSnrc (Kawrakow and Rogers 2003) for the particle transport and scoring of the energy depositions. EGSnrc is a variant of EGS4 (Nelson *et al* 1985) with improved

[1] In the EGS language the problem-specific parts of the complete Monte Carlo programme, which have to be developed by the user, are called 'user codes'.

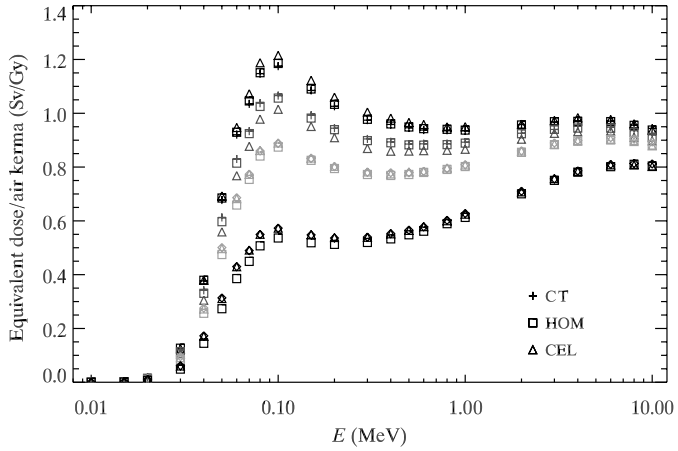

Figure 1. Comparison of mean RBM dose conversion coefficients in Godwin for different treatments of the bones, where 'CT' denotes the heterogeneous bones derived from CT grey values and 'HOM' its homogenized variant. For 'CEL' the RBM distribution is also homogenous in each bone, but has been adjusted to agree with the data of ICRP (1995, 2002). The total amount of red and yellow bone marrow and mineral bone is the same in all models. The symbol groups correspond from top to bottom to PA, AP, ROT and LLAT exposure.

physics and electron transport algorithm. In particular, bound Compton scattering and photo-electrons from K, L and M shells are included. For both effects, resulting fluorescence or Auger and Coster–Kronig electrons are taken into account. The originally used EGS4 input data for photon cross sections have been updated by Seuntjens *et al* (2002). With the help of the XCOM program (Berger and Hubbell 1987) they obtained improved cross sections for photo-effect, Rayleigh scattering and pair production in agreement with the NIST/XCOM database, and transferred the results in a format accessible by EGS.

The electron collision stopping powers have been revised to the values recommended by ICRU (1984). A new multiple scattering theory including spin effects has been implemented as well as an improved transport algorithm for electrons (PRESTA-II, Kawrakow and Bielajew (1998)).

In the computations of this work, the tracks of primary and secondary photons are followed down to kinetic energies of 2 keV, those of secondary electrons down to 20 keV. It has been shown that the dose conversion coefficients obtained with our user code are in very good agreement with the values obtained by Taranenko *et al* (2005) with MCNPX (Hendricks *et al* 2005), except for photon energies below about 50 keV. The discrepancies at low energies have been caused by the, at that time, standard MCPLIB02 cross-section library of MCNP, which showed shortcomings in the cross section for the photo-electric effect for low energies and low Z material. By employing the updated, now standard, MCPLIB04 library of MCNPX, which conforms to the data of the more recent EPDL97 compilation (Cullen *et al* 1997), the cross sections used in MCNPX and EGSnrc are now almost identical. As a result, the dose conversion coefficients computed with MCNPX and EGSnrc agree now within the statistical uncertainties (Taranenko 2005).

The huge increase in computational power in the last few years allows the computation of organ dose conversion coefficients with low statistical uncertainties. Nevertheless, for tiny organs such as eye lenses, good results in their dose conversion coefficients can only be obtained with disproportionally high additional effort. Therefore, importance sampling

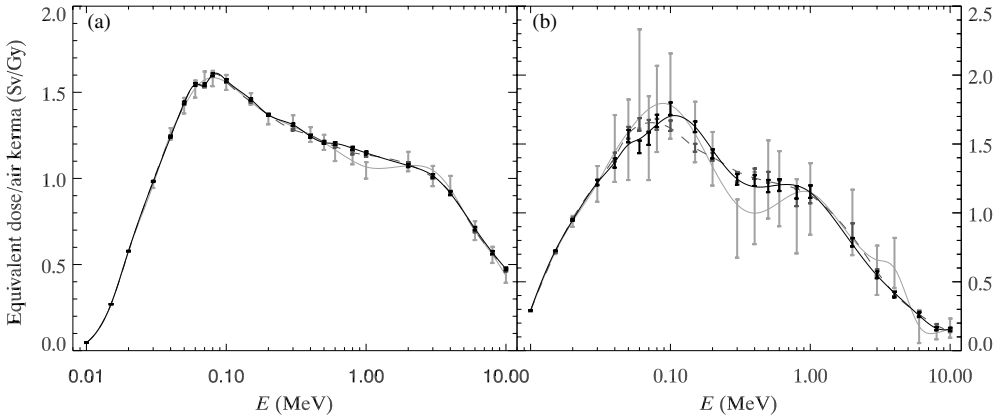

Figure 2. Comparison of dose conversion coefficients for eyes (a) and eye lenses (b) computed without (grey) and with (black) importance sampling for the eyes of Rex in AP geometry. The error bars indicate the 2σ statistical uncertainties with the mean value at their centre. The curves are drawn for guidance. The light grey bars (connected by the dash-dotted line) show the results with the standard number of histories, while for the dark grey bars (dashed) 50 times more particles were used, i.e., varying from 1 billion at 10 keV to 375 million at 10 MeV. For the importance sampling case (black bars), the same particle excess was employed, but only in the region around the eyes.

has been implemented into the code to increase the number of photons considerably in those source regions, from where the photons are directed at the organs of interest. Simultaneously, the statistical weight of those photons is decreased appropriately. For the particle density in the (rectangular) 'regions of interest', the Cauchy (Lorenzian) probability density function has been chosen. In general, a scheme similar to that described by Ulanovsky *et al* (2005) is followed, which has been applied successfully for human tooth dosimetry.

The implementation of importance sampling has been verified for one exemplary case, where the organs of interest were the eyes and eye lenses of Rex in antero-posterior exposure. In the first simulation, the number of particle histories was 50 times higher than in our standard case (see section 3) throughout the whole irradiation plane (dark grey bars in figure 2). The resulting dose conversion coefficients have been compared with a second simulation using importance sampling, i.e., where solely in the source region directly irradiating the eyes the history density was on average 50-fold enhanced compared to the rest of the source plane (black bars). Within the statistical uncertainty, the same results have been obtained for both cases confirming the validity of the importance-sampling algorithm (figure 2). With the total particle number in the second simulation being only about 10% higher than in the standard case, the advantage of importance sampling is obvious. It could also be attested that the dose conversion coefficients of neighbouring organs are not modified by the algorithm.

3. Dose conversion coefficients for idealized external photon exposures

With the Monte Carlo code, dose conversion coefficients for idealized external exposures have been computed as equivalent dose per air kerma free in air in the entrance plane. (For photons, equivalent dose is numerically equal to absorbed dose.) The standard irradiation geometries investigated were antero-posterior (AP), postero-anterior (PA), left- (LLAT) and right-side lateral (RLAT), rotational (ROT) and isotropic (ISO) monoenergetic sources. The number of source photons followed in the Monte Carlo simulations decreased from 20 million at 10 keV

Table 2. Tissue weighting factors (w_T) for the computation of the effective dose as given by the draft recommendations of ICRP (2006). The dose conversion coefficient of the remainder tissues is obtained as the arithmetic mean of the conversion coefficients of their constituents (see the footnote).

Tissue	w_T
Active bone marrow, colon, lung, stomach, glandular breast tissue, remainder tissues[a]	0.12
Gonads	0.08
Urinary bladder, oesophagus, liver, thyroid	0.04
Bone surface, brain, salivary glands, skin	0.01

[a] Adrenals, extrathoracic (ET) region, gall bladder, heart, kidneys, lymphatic nodes, muscle, oral mucosa, pancreas, prostate/uterus, small intestine, spleen, thymus.

to 7.5 million at 10 MeV. Thus, the dose conversion coefficients of large organs could be determined in all geometries with statistical uncertainties of at most around 0.2%; for smaller organs, the statistical uncertainties were around 1%, in most cases even less. Importance sampling was used to reach this statistical uncertainty level also in the smallest organs. In detail, the number of particles irradiating gall bladder, prostate, testes, ovaries, thymus and thyroid was enhanced by a factor of five, while the number of photons in the region of the glandular breast tissue and adrenals was ten times higher than outside this area.

Around the eyes, the number of histories was increased by a factor of 50. Thereby the statistical uncertainties for the eye lenses could be decreased to around 2% for all exposures, apart from PA and ISO. In PA, only a low number of photons were able to penetrate the skull and enter the eyes lenses, which led to uncertainties ranging from 10% at 40 keV to 1% at 10 MeV. In isotropic geometry no importance sampling has been employed which led to statistical uncertainties for the eye lenses of about 12%, for small organs of about 4%.

The overall accuracy of the dose conversion coefficients is certainly limited by uncertainties in the physical input parameters, like photon cross sections, and deviations of the particle transport simulation from 'real physics', which exceed the statistical uncertainties. Furthermore, it should be stressed that the presented dose conversion coefficients are for the average human; they certainly can differ much more than the aforementioned uncertainties from the values in individual persons.

A list of all organs contributing to the effective dose as defined in the ICRP draft recommendations (ICRP 2006) is provided in table 2, together with their respective tissue weighting factors and the organs contributing to the so-called remainder. The organ dose conversion coefficients given as equivalent dose per air kerma free in air in the entrance plane for the organs having a specific tissue weighting factor are summarized in tables 3–10.[2] Table 10 contains conversion coefficients for the eye lenses, too. The resulting effective dose conversion coefficients are given in table 11.

4. Discussion

4.1. Comparison with ICRP Publication 74 (ICRP 1996)

The organ dose conversion coefficients of Rex and Regina have been compared to the values of ICRP Publication 74 (ICRP 1996), which have been derived with mathematical models. In addition to the obvious anatomical differences in the models, the present computations differ

[2] The dose conversion coefficients for any organ of Rex and Regina are available electronically from the authors or, in the near future, from a web interface at http://www.gsf.de.

Table 3. Organ equivalent dose conversion coefficients in Sv Gy^{-1} of active bone marrow and brain for standard idealized external exposure geometries.

Energy	AP		PA		LLAT		RLAT		ROT		ISO	
(MeV)	Rex	Regina	Rex	Regina	Rex	Regina	Rex	Regina	Rex	Regina	Rex	Regina
						Active bone marrow						
0.010	0.000	0.000	0.000	0.000	0.000	0.000	0.000	0.000	0.000	0.000	0.000	0.000
0.015	0.004	0.003	0.000	0.002	0.001	0.002	0.001	0.001	0.002	0.002	0.002	0.002
0.020	0.019	0.020	0.007	0.017	0.007	0.009	0.008	0.009	0.010	0.014	0.009	0.011
0.030	0.118	0.140	0.106	0.153	0.052	0.060	0.054	0.063	0.084	0.107	0.067	0.083
0.040	0.329	0.388	0.352	0.434	0.152	0.175	0.156	0.182	0.256	0.306	0.199	0.239
0.050	0.583	0.671	0.654	0.753	0.279	0.319	0.286	0.331	0.471	0.544	0.368	0.425
0.060	0.789	0.896	0.904	1.000	0.388	0.436	0.398	0.451	0.651	0.727	0.508	0.576
0.070	0.887	0.989	0.026	1.103	0.445	0.495	0.456	0.512	0.743	0.817	0.586	0.647
0.080	0.987	1.090	0.138	1.209	0.502	0.551	0.512	0.569	0.830	0.901	0.651	0.714
0.100	1.021	1.102	0.179	1.223	0.530	0.574	0.540	0.592	0.862	0.919	0.684	0.735
0.150	0.961	1.023	0.109	1.128	0.520	0.559	0.529	0.572	0.826	0.863	0.657	0.697
0.200	0.926	0.973	0.051	1.065	0.515	0.553	0.525	0.565	0.795	0.830	0.643	0.671
0.300	0.888	0.930	0.007	1.010	0.523	0.562	0.532	0.571	0.780	0.809	0.636	0.666
0.400	0.878	0.914	0.981	0.982	0.539	0.577	0.546	0.586	0.778	0.804	0.640	0.668
0.500	0.876	0.909	0.967	0.973	0.554	0.592	0.560	0.602	0.779	0.807	0.649	0.677
0.600	0.875	0.905	0.962	0.964	0.569	0.606	0.577	0.613	0.786	0.816	0.660	0.685
0.800	0.875	0.906	0.953	0.960	0.596	0.635	0.603	0.641	0.799	0.822	0.678	0.706
1.000	0.882	0.912	0.948	0.961	0.621	0.658	0.627	0.665	0.812	0.833	0.695	0.725
2.000	0.918	0.942	0.967	0.974	0.710	0.745	0.713	0.753	0.863	0.881	0.767	0.794
3.000	0.938	0.962	0.977	0.988	0.761	0.795	0.760	0.800	0.890	0.912	0.808	0.830
4.000	0.952	0.975	0.989	0.998	0.795	0.828	0.795	0.827	0.912	0.929	0.837	0.856
6.000	0.962	0.973	1.000	1.002	0.827	0.851	0.829	0.854	0.925	0.947	0.859	0.877
8.000	0.943	0.964	0.991	0.991	0.833	0.859	0.835	0.862	0.921	0.943	0.862	0.879
10.000	0.929	0.947	0.984	0.973	0.838	0.857	0.838	0.859	0.921	0.934	0.860	0.871
						Brain						
0.010	0.000	0.000	0.000	0.000	0.000	0.000	0.000	0.000	0.000	0.000	0.000	0.000
0.015	0.000	0.000	0.000	0.000	0.000	0.000	0.000	0.000	0.000	0.000	0.000	0.000
0.020	0.001	0.001	0.001	0.002	0.003	0.004	0.003	0.004	0.002	0.003	0.003	0.004
0.030	0.052	0.062	0.077	0.094	0.107	0.131	0.110	0.134	0.088	0.106	0.088	0.100
0.040	0.222	0.252	0.304	0.333	0.382	0.428	0.392	0.432	0.329	0.367	0.303	0.334
0.050	0.426	0.470	0.546	0.574	0.658	0.708	0.677	0.715	0.577	0.623	0.532	0.566
0.060	0.580	0.624	0.719	0.744	0.848	0.894	0.868	0.896	0.761	0.798	0.684	0.719
0.070	0.645	0.692	0.786	0.799	0.918	0.953	0.937	0.958	0.826	0.860	0.748	0.775
0.080	0.712	0.757	0.852	0.860	0.989	1.020	1.008	1.027	0.897	0.925	0.809	0.837
0.100	0.740	0.780	0.863	0.870	0.993	1.017	1.013	1.023	0.914	0.929	0.826	0.845
0.150	0.725	0.755	0.829	0.839	0.943	0.967	0.957	0.969	0.872	0.896	0.794	0.807
0.200	0.716	0.745	0.810	0.824	0.915	0.940	0.926	0.941	0.849	0.869	0.771	0.791
0.300	0.723	0.744	0.802	0.812	0.897	0.916	0.904	0.922	0.841	0.860	0.768	0.786
0.400	0.733	0.756	0.805	0.815	0.890	0.912	0.901	0.919	0.835	0.856	0.771	0.792
0.500	0.746	0.763	0.811	0.824	0.893	0.915	0.903	0.913	0.843	0.858	0.772	0.795
0.600	0.756	0.769	0.820	0.828	0.897	0.912	0.902	0.915	0.851	0.866	0.788	0.807
0.800	0.776	0.798	0.837	0.841	0.902	0.919	0.906	0.930	0.859	0.877	0.805	0.819
1.000	0.799	0.814	0.852	0.860	0.909	0.931	0.918	0.929	0.872	0.895	0.816	0.832
2.000	0.866	0.874	0.899	0.914	0.948	0.963	0.952	0.965	0.923	0.927	0.876	0.885
3.000	0.906	0.905	0.928	0.944	0.970	0.983	0.971	0.979	0.947	0.955	0.903	0.910
4.000	0.920	0.932	0.944	0.948	0.975	0.991	0.977	0.992	0.968	0.975	0.919	0.926
6.000	0.935	0.947	0.965	0.981	0.985	0.997	1.002	1.002	0.976	0.986	0.944	0.941
8.000	0.948	0.958	0.970	0.972	0.996	0.997	0.987	0.991	0.991	0.971	0.943	0.956
10.000	0.955	0.954	0.969	0.968	0.980	0.980	0.979	0.978	0.968	0.973	0.947	0.948

Table 4. Organ equivalent dose conversion coefficients in Sv Gy^{-1} of spongiosa (substitute for bone surface) and glandular tissue of the breasts.

Energy	AP		PA		LLAT		RLAT		ROT		ISO	
(MeV)	Rex	Regina	Rex	Regina	Rex	Regina	Rex	Regina	Rex	Regina	Rex	Regina
						Spongiosa						
0.010	0.000	0.000	0.000	0.000	0.000	0.000	0.000	0.000	0.000	0.000	0.000	0.000
0.015	0.003	0.004	0.001	0.002	0.002	0.002	0.002	0.002	0.003	0.003	0.004	0.004
0.020	0.035	0.043	0.020	0.032	0.022	0.027	0.023	0.027	0.028	0.035	0.029	0.033
0.030	0.331	0.378	0.264	0.329	0.199	0.226	0.203	0.229	0.265	0.308	0.224	0.251
0.040	0.826	0.913	0.732	0.841	0.483	0.545	0.487	0.550	0.671	0.757	0.556	0.616
0.050	1.247	1.355	0.154	1.286	0.726	0.817	0.732	0.823	1.029	1.138	0.849	0.930
0.060	1.474	1.586	0.398	1.528	0.859	0.961	0.867	0.967	1.221	1.336	1.012	1.097
0.070	1.480	1.577	0.432	1.536	0.869	0.962	0.874	0.968	1.240	1.344	1.030	1.101
0.080	1.503	1.595	0.467	1.556	0.885	0.969	0.891	0.976	1.265	1.354	1.049	1.112
0.100	1.374	1.436	0.356	1.411	0.818	0.880	0.823	0.888	1.163	1.229	0.970	1.012
0.150	1.143	1.180	0.141	1.167	0.700	0.742	0.705	0.746	0.984	1.017	0.821	0.847
0.200	1.050	1.075	0.045	1.064	0.658	0.693	0.662	0.695	0.906	0.935	0.767	0.779
0.300	0.974	0.994	0.977	0.989	0.637	0.669	0.641	0.671	0.859	0.880	0.730	0.743
0.400	0.949	0.966	0.951	0.959	0.639	0.669	0.644	0.671	0.843	0.864	0.726	0.736
0.500	0.939	0.956	0.940	0.949	0.646	0.677	0.649	0.680	0.839	0.859	0.728	0.741
0.600	0.938	0.948	0.936	0.944	0.656	0.686	0.659	0.686	0.840	0.863	0.738	0.746
0.800	0.931	0.944	0.933	0.940	0.676	0.705	0.678	0.707	0.851	0.866	0.750	0.764
1.000	0.934	0.948	0.930	0.942	0.694	0.724	0.696	0.724	0.858	0.874	0.761	0.778
2.000	0.957	0.968	0.957	0.963	0.766	0.794	0.765	0.795	0.900	0.914	0.823	0.834
3.000	0.975	0.987	0.973	0.980	0.810	0.837	0.808	0.836	0.924	0.938	0.856	0.869
4.000	0.986	0.997	0.988	0.994	0.838	0.863	0.838	0.862	0.942	0.953	0.880	0.892
6.000	0.987	0.990	0.998	1.004	0.863	0.882	0.864	0.882	0.952	0.965	0.896	0.908
8.000	0.969	0.981	0.990	0.988	0.864	0.887	0.863	0.886	0.944	0.957	0.898	0.906
10.000	0.949	0.958	0.981	0.971	0.857	0.879	0.857	0.877	0.933	0.944	0.889	0.895
						Breast, glandular tissue						
0.010	0.099	0.012	0.000	0.000	0.020	0.003	0.015	0.004	0.036	0.005	0.030	0.004
0.015	0.444	0.134	0.000	0.000	0.144	0.044	0.126	0.045	0.174	0.056	0.152	0.046
0.020	0.712	0.376	0.000	0.000	0.285	0.136	0.265	0.138	0.316	0.167	0.287	0.143
0.030	1.047	0.838	0.007	0.037	0.464	0.353	0.444	0.350	0.503	0.405	0.489	0.363
0.040	1.269	1.179	0.053	0.155	0.582	0.533	0.560	0.524	0.644	0.609	0.605	0.542
0.050	1.445	1.411	0.122	0.300	0.689	0.668	0.651	0.654	0.796	0.759	0.727	0.676
0.060	1.585	1.545	0.207	0.412	0.761	0.752	0.750	0.737	0.831	0.868	0.783	0.768
0.070	1.562	1.547	0.255	0.468	0.766	0.774	0.733	0.757	0.866	0.894	0.780	0.791
0.080	1.624	1.607	0.282	0.526	0.799	0.823	0.777	0.802	0.931	0.945	0.872	0.837
0.100	1.555	1.561	0.339	0.576	0.826	0.827	0.778	0.810	0.936	0.951	0.910	0.846
0.150	1.463	1.430	0.387	0.602	0.802	0.813	0.774	0.797	0.886	0.910	0.874	0.811
0.200	1.398	1.357	0.410	0.621	0.766	0.805	0.779	0.793	0.891	0.893	0.839	0.795
0.300	1.341	1.273	0.488	0.658	0.771	0.806	0.756	0.798	0.888	0.873	0.840	0.797
0.400	1.256	1.222	0.515	0.690	0.772	0.812	0.744	0.803	0.856	0.870	0.843	0.774
0.500	1.208	1.184	0.541	0.714	0.783	0.823	0.753	0.816	0.848	0.875	0.846	0.795
0.600	1.215	1.170	0.563	0.742	0.781	0.831	0.777	0.820	0.865	0.875	0.915	0.805
0.800	1.214	1.145	0.655	0.778	0.796	0.847	0.778	0.837	0.896	0.887	0.822	0.815
1.000	1.158	1.121	0.708	0.803	0.810	0.862	0.788	0.859	0.884	0.898	0.858	0.814
2.000	0.966	1.097	0.774	0.873	0.822	0.921	0.816	0.909	0.867	0.924	0.847	0.872
3.000	0.737	1.053	0.824	0.909	0.785	0.937	0.767	0.931	0.810	0.939	0.802	0.881
4.000	0.568	1.007	0.842	0.924	0.756	0.936	0.751	0.928	0.772	0.934	0.694	0.876
6.000	0.387	0.877	0.840	0.938	0.660	0.909	0.668	0.899	0.637	0.892	0.599	0.855
8.000	0.275	0.754	0.893	0.930	0.591	0.865	0.616	0.858	0.588	0.834	0.584	0.824
10.000	0.225	0.641	0.892	0.921	0.570	0.825	0.572	0.818	0.541	0.785	0.519	0.774

Table 5. Organ equivalent dose conversion coefficients in Sv Gy^{-1} of colon and gonads.

Energy	AP		PA		LLAT		RLAT		ROT		ISO	
(MeV)	Rex	Regina	Rex	Regina	Rex	Regina	Rex	Regina	Rex	Regina	Rex	Regina
						Colon						
0.010	0.000	0.000	0.000	0.000	0.000	0.000	0.000	0.000	0.000	0.000	0.000	0.000
0.015	0.005	0.012	0.000	0.000	0.002	0.000	0.000	0.000	0.002	0.003	0.001	0.002
0.020	0.052	0.102	0.003	0.007	0.029	0.010	0.012	0.011	0.022	0.032	0.015	0.021
0.030	0.367	0.507	0.086	0.105	0.207	0.109	0.128	0.115	0.187	0.211	0.136	0.151
0.040	0.788	0.965	0.298	0.315	0.432	0.277	0.314	0.286	0.443	0.464	0.331	0.350
0.050	1.137	1.327	0.540	0.559	0.623	0.442	0.491	0.441	0.685	0.698	0.512	0.532
0.060	1.372	1.535	0.725	0.741	0.743	0.557	0.602	0.555	0.837	0.861	0.638	0.656
0.070	1.419	1.570	0.803	0.814	0.777	0.600	0.638	0.593	0.896	0.910	0.685	0.697
0.080	1.475	1.623	0.875	0.888	0.816	0.646	0.679	0.640	0.950	0.962	0.738	0.743
0.100	1.415	1.561	0.896	0.897	0.804	0.652	0.674	0.643	0.932	0.937	0.731	0.739
0.150	1.248	1.381	0.835	0.836	0.744	0.621	0.627	0.612	0.862	0.875	0.673	0.676
0.200	1.171	1.281	0.809	0.810	0.718	0.611	0.616	0.598	0.819	0.838	0.648	0.654
0.300	1.085	1.183	0.789	0.791	0.702	0.615	0.613	0.608	0.792	0.811	0.629	0.645
0.400	1.051	1.126	0.793	0.783	0.702	0.630	0.618	0.619	0.784	0.804	0.632	0.646
0.500	1.027	1.096	0.798	0.805	0.713	0.647	0.630	0.638	0.781	0.801	0.638	0.654
0.600	1.021	1.083	0.799	0.801	0.717	0.660	0.641	0.650	0.783	0.798	0.649	0.664
0.800	1.003	1.069	0.800	0.802	0.737	0.686	0.665	0.675	0.796	0.814	0.670	0.688
1.000	1.005	1.047	0.813	0.816	0.742	0.706	0.686	0.696	0.814	0.835	0.688	0.691
2.000	0.995	1.036	0.873	0.868	0.816	0.783	0.771	0.778	0.856	0.885	0.740	0.763
3.000	1.002	1.034	0.893	0.898	0.854	0.828	0.809	0.826	0.880	0.911	0.796	0.805
4.000	1.018	1.048	0.913	0.904	0.873	0.848	0.840	0.842	0.913	0.918	0.814	0.831
6.000	0.998	1.029	0.941	0.938	0.890	0.890	0.856	0.876	0.931	0.922	0.857	0.861
8.000	1.006	1.004	0.936	0.937	0.898	0.884	0.882	0.879	0.924	0.934	0.864	0.885
10.000	0.984	0.982	0.952	0.949	0.889	0.893	0.870	0.902	0.935	0.927	0.862	0.872
						Gonads						
0.010	0.007	0.000	0.000	0.000	0.000	0.000	0.000	0.000	0.004	0.000	0.006	0.000
0.015	0.083	0.000	0.000	0.000	0.000	0.000	0.000	0.000	0.037	0.000	0.037	0.000
0.020	0.281	0.002	0.003	0.008	0.002	0.000	0.001	0.000	0.119	0.002	0.107	0.001
0.030	0.845	0.112	0.090	0.197	0.038	0.005	0.020	0.006	0.352	0.077	0.310	0.051
0.040	1.341	0.427	0.305	0.561	0.130	0.057	0.086	0.068	0.596	0.268	0.508	0.194
0.050	1.680	0.730	0.500	0.890	0.237	0.146	0.181	0.162	0.789	0.515	0.677	0.350
0.060	1.855	0.987	0.642	1.137	0.319	0.233	0.246	0.276	0.904	0.743	0.779	0.518
0.070	1.843	1.068	0.724	1.272	0.358	0.308	0.287	0.336	0.944	0.802	0.777	0.589
0.080	1.862	1.201	0.770	1.376	0.395	0.339	0.326	0.402	0.967	0.844	0.834	0.675
0.100	1.773	1.208	0.779	1.337	0.409	0.375	0.335	0.432	0.947	0.830	0.824	0.674
0.150	1.539	1.057	0.719	1.169	0.427	0.391	0.359	0.438	0.861	0.785	0.752	0.589
0.200	1.409	1.016	0.724	1.080	0.431	0.383	0.377	0.438	0.836	0.734	0.741	0.603
0.300	1.281	0.982	0.742	1.003	0.471	0.402	0.413	0.454	0.802	0.725	0.684	0.599
0.400	1.213	0.972	0.757	0.968	0.493	0.448	0.454	0.474	0.805	0.729	0.688	0.571
0.500	1.196	0.933	0.767	0.973	0.521	0.467	0.492	0.504	0.797	0.716	0.686	0.583
0.600	1.166	0.940	0.786	0.947	0.545	0.471	0.504	0.505	0.809	0.761	0.734	0.596
0.800	1.125	0.902	0.789	0.946	0.591	0.507	0.560	0.544	0.834	0.760	0.733	0.661
1.000	1.100	0.913	0.805	1.008	0.631	0.571	0.587	0.597	0.821	0.761	0.700	0.696
2.000	1.075	0.968	0.870	0.942	0.740	0.653	0.718	0.695	0.863	0.839	0.819	0.778
3.000	1.041	0.982	0.928	0.994	0.799	0.724	0.763	0.757	0.882	0.896	0.818	0.817
4.000	1.016	0.950	0.906	0.974	0.826	0.752	0.802	0.772	0.882	0.882	0.854	0.869
6.000	0.923	0.986	0.946	1.016	0.851	0.805	0.830	0.829	0.891	0.911	0.839	0.727
8.000	0.851	0.968	0.936	1.021	0.867	0.796	0.847	0.829	0.838	0.873	0.816	0.841
10.000	0.778	0.939	0.937	1.002	0.856	0.825	0.831	0.862	0.839	0.925	0.773	0.865

Table 6. Organ equivalent dose conversion coefficients in Sv Gy^{-1} of liver and lungs.

Energy	AP		PA		LLAT		RLAT		ROT		ISO	
(MeV)	Rex	Regina	Rex	Regina	Rex	Regina	Rex	Regina	Rex	Regina	Rex	Regina
						Liver						
0.010	0.000	0.000	0.000	0.000	0.000	0.000	0.000	0.000	0.000	0.000	0.000	0.000
0.015	0.001	0.004	0.000	0.001	0.000	0.000	0.001	0.002	0.001	0.002	0.000	0.001
0.020	0.022	0.047	0.004	0.014	0.000	0.003	0.019	0.028	0.011	0.023	0.007	0.014
0.030	0.218	0.333	0.081	0.146	0.011	0.041	0.179	0.216	0.119	0.181	0.085	0.127
0.040	0.560	0.737	0.279	0.402	0.059	0.135	0.456	0.499	0.334	0.440	0.251	0.323
0.050	0.887	1.080	0.524	0.670	0.132	0.245	0.716	0.747	0.562	0.688	0.433	0.513
0.060	1.112	1.296	0.719	0.865	0.199	0.332	0.897	0.906	0.728	0.855	0.568	0.645
0.070	1.182	1.344	0.816	0.946	0.237	0.376	0.953	0.951	0.796	0.908	0.620	0.694
0.080	1.257	1.409	0.893	1.016	0.275	0.416	1.019	1.005	0.865	0.969	0.679	0.740
0.100	1.232	1.362	0.919	1.020	0.296	0.434	1.011	0.989	0.869	0.960	0.687	0.741
0.150	1.105	1.219	0.866	0.947	0.308	0.434	0.939	0.920	0.807	0.885	0.640	0.691
0.200	1.035	1.139	0.831	0.906	0.319	0.441	0.897	0.885	0.772	0.849	0.622	0.669
0.300	0.972	1.070	0.803	0.870	0.344	0.463	0.870	0.865	0.747	0.822	0.613	0.655
0.400	0.942	1.029	0.800	0.861	0.374	0.492	0.864	0.861	0.744	0.813	0.616	0.656
0.500	0.930	1.013	0.799	0.857	0.398	0.512	0.862	0.860	0.750	0.813	0.626	0.668
0.600	0.923	1.000	0.806	0.858	0.424	0.533	0.863	0.869	0.751	0.812	0.632	0.671
0.800	0.918	0.991	0.814	0.862	0.465	0.570	0.870	0.879	0.766	0.826	0.656	0.694
1.000	0.913	0.979	0.826	0.869	0.500	0.602	0.880	0.890	0.780	0.835	0.667	0.713
2.000	0.935	1.000	0.869	0.906	0.615	0.704	0.919	0.929	0.837	0.882	0.744	0.783
3.000	0.962	0.999	0.888	0.931	0.681	0.760	0.940	0.951	0.866	0.910	0.796	0.822
4.000	0.968	1.001	0.913	0.941	0.720	0.794	0.952	0.960	0.886	0.928	0.815	0.848
6.000	0.976	1.015	0.927	0.946	0.765	0.828	0.965	0.975	0.903	0.949	0.846	0.869
8.000	0.960	1.005	0.927	0.956	0.789	0.843	0.968	0.975	0.917	0.946	0.855	0.892
10.000	0.969	0.985	0.931	0.950	0.796	0.853	0.958	0.962	0.914	0.941	0.862	0.892
						Lungs						
0.010	0.000	0.000	0.000	0.000	0.000	0.000	0.000	0.000	0.000	0.000	0.000	0.000
0.015	0.003	0.002	0.000	0.002	0.000	0.001	0.000	0.001	0.001	0.001	0.000	0.001
0.020	0.042	0.034	0.005	0.033	0.004	0.010	0.003	0.012	0.013	0.022	0.009	0.014
0.030	0.307	0.294	0.113	0.281	0.050	0.075	0.050	0.090	0.135	0.193	0.101	0.142
0.040	0.667	0.660	0.381	0.665	0.154	0.202	0.156	0.224	0.357	0.463	0.281	0.361
0.050	0.973	0.975	0.680	1.007	0.276	0.337	0.277	0.359	0.582	0.713	0.469	0.563
0.060	1.165	1.161	0.906	1.223	0.374	0.434	0.372	0.457	0.746	0.878	0.609	0.698
0.070	1.227	1.204	1.005	1.291	0.419	0.476	0.416	0.494	0.810	0.931	0.667	0.743
0.080	1.298	1.263	1.098	1.367	0.460	0.518	0.457	0.532	0.878	0.983	0.721	0.799
0.100	1.266	1.229	1.112	1.344	0.476	0.524	0.474	0.538	0.885	0.976	0.734	0.792
0.150	1.153	1.111	1.045	1.223	0.467	0.510	0.463	0.522	0.830	0.905	0.693	0.741
0.200	1.097	1.048	0.998	1.158	0.465	0.509	0.465	0.520	0.807	0.870	0.677	0.719
0.300	1.042	0.996	0.961	1.094	0.481	0.524	0.477	0.530	0.788	0.844	0.669	0.712
0.400	1.020	0.979	0.941	1.069	0.501	0.546	0.496	0.551	0.784	0.841	0.674	0.713
0.500	1.007	0.972	0.939	1.052	0.520	0.567	0.515	0.570	0.786	0.845	0.688	0.721
0.600	0.993	0.960	0.940	1.040	0.538	0.587	0.534	0.585	0.788	0.846	0.696	0.734
0.800	0.982	0.958	0.933	1.025	0.577	0.618	0.561	0.618	0.808	0.855	0.717	0.750
1.000	0.985	0.960	0.941	1.024	0.598	0.650	0.592	0.645	0.817	0.872	0.731	0.768
2.000	0.993	0.984	0.961	1.028	0.699	0.741	0.693	0.736	0.872	0.910	0.803	0.829
3.000	1.014	0.999	0.983	1.031	0.758	0.799	0.745	0.794	0.898	0.941	0.839	0.865
4.000	1.017	1.011	0.990	1.036	0.791	0.836	0.787	0.822	0.922	0.959	0.863	0.894
6.000	1.025	1.017	1.000	1.037	0.830	0.865	0.828	0.868	0.956	0.977	0.892	0.905
8.000	1.027	1.019	1.019	1.046	0.857	0.893	0.853	0.883	0.952	0.987	0.912	0.936
10.000	0.999	1.015	1.021	1.028	0.866	0.901	0.866	0.898	0.960	0.990	0.914	0.930

Table 7. Organ equivalent dose conversion coefficients in Sv Gy^{-1} of oesophagus and salivary glands.

Energy	AP		PA		LLAT		RLAT		ROT		ISO	
(MeV)	Rex	Regina	Rex	Regina	Rex	Regina	Rex	Regina	Rex	Regina	Rex	Regina
						Oesophagus						
0.010	0.000	0.000	0.000	0.000	0.000	0.000	0.000	0.000	0.000	0.000	0.000	0.000
0.015	0.004	0.004	0.000	0.000	0.000	0.000	0.000	0.000	0.001	0.001	0.000	0.000
0.020	0.035	0.041	0.000	0.001	0.005	0.002	0.003	0.002	0.011	0.012	0.006	0.006
0.030	0.215	0.261	0.030	0.070	0.051	0.032	0.042	0.039	0.093	0.116	0.057	0.074
0.040	0.507	0.598	0.198	0.301	0.149	0.137	0.123	0.133	0.270	0.322	0.183	0.227
0.050	0.810	0.883	0.472	0.624	0.275	0.259	0.233	0.254	0.470	0.564	0.345	0.408
0.060	1.004	1.108	0.695	0.850	0.387	0.376	0.326	0.339	0.633	0.755	0.474	0.547
0.070	1.071	1.185	0.813	0.970	0.431	0.438	0.372	0.392	0.745	0.807	0.540	0.626
0.080	1.201	1.282	0.946	1.063	0.488	0.479	0.421	0.454	0.823	0.903	0.605	0.701
0.100	1.197	1.260	1.000	1.081	0.520	0.503	0.456	0.472	0.828	0.905	0.649	0.707
0.150	1.115	1.174	0.951	1.050	0.518	0.503	0.465	0.479	0.812	0.878	0.635	0.691
0.200	1.061	1.115	0.878	0.985	0.522	0.500	0.463	0.488	0.784	0.846	0.614	0.664
0.300	0.995	1.046	0.913	0.942	0.539	0.521	0.483	0.500	0.765	0.825	0.616	0.670
0.400	0.997	1.030	0.887	0.938	0.557	0.553	0.502	0.509	0.788	0.816	0.601	0.660
0.500	0.986	1.016	0.867	0.915	0.567	0.561	0.527	0.535	0.791	0.837	0.624	0.666
0.600	0.941	1.004	0.868	0.919	0.600	0.577	0.537	0.560	0.776	0.827	0.654	0.671
0.800	0.947	0.982	0.857	0.898	0.627	0.624	0.569	0.598	0.808	0.829	0.646	0.707
1.000	0.962	0.997	0.884	0.921	0.641	0.617	0.599	0.613	0.805	0.856	0.684	0.719
2.000	0.977	0.999	0.914	0.961	0.736	0.742	0.691	0.740	0.866	0.907	0.754	0.797
3.000	0.975	1.051	0.917	0.947	0.807	0.804	0.751	0.756	0.873	0.951	0.798	0.809
4.000	0.994	1.028	0.941	0.982	0.827	0.831	0.810	0.811	0.921	0.960	0.799	0.826
6.000	1.013	1.009	0.952	0.967	0.841	0.872	0.837	0.856	0.962	0.993	0.885	0.874
8.000	0.984	0.987	0.965	1.004	0.854	0.872	0.812	0.846	0.978	0.947	0.855	0.915
10.000	0.968	0.988	0.985	1.012	0.881	0.882	0.864	0.906	0.955	0.983	0.864	0.921
						Salivary glands						
0.010	0.000	0.000	0.001	0.000	0.010	0.004	0.007	0.003	0.004	0.002	0.003	0.001
0.015	0.010	0.003	0.022	0.008	0.101	0.068	0.087	0.063	0.060	0.038	0.042	0.025
0.020	0.075	0.032	0.101	0.059	0.234	0.189	0.219	0.186	0.166	0.123	0.123	0.087
0.030	0.328	0.215	0.331	0.273	0.468	0.430	0.444	0.436	0.395	0.347	0.306	0.257
0.040	0.579	0.456	0.559	0.520	0.662	0.649	0.640	0.666	0.602	0.574	0.472	0.414
0.050	0.778	0.667	0.739	0.725	0.816	0.834	0.805	0.859	0.767	0.762	0.617	0.579
0.060	0.915	0.844	0.875	0.865	0.941	0.969	0.919	0.989	0.890	0.926	0.716	0.688
0.070	0.971	0.917	0.896	0.938	0.951	1.005	0.954	1.014	0.943	0.963	0.736	0.715
0.080	1.027	0.970	0.982	0.991	1.022	1.071	1.021	1.081	0.988	1.036	0.795	0.774
0.100	1.058	0.979	1.009	1.025	1.033	1.097	1.025	1.085	1.016	1.069	0.817	0.821
0.150	1.047	0.982	1.014	0.987	0.992	1.037	0.982	1.032	0.966	1.040	0.793	0.790
0.200	1.019	0.957	0.993	0.999	0.959	1.015	0.955	1.019	0.966	1.017	0.785	0.777
0.300	0.980	0.919	0.979	0.988	0.934	1.005	0.926	0.987	0.942	0.971	0.788	0.762
0.400	0.999	0.932	1.007	0.986	0.927	0.973	0.909	0.963	0.932	0.959	0.791	0.769
0.500	1.011	0.933	0.993	0.980	0.934	0.983	0.906	0.967	0.940	0.985	0.781	0.794
0.600	0.999	0.960	0.998	0.984	0.946	0.986	0.926	0.983	0.945	0.978	0.814	0.801
0.800	0.984	0.941	1.018	1.002	0.938	0.966	0.925	0.984	0.938	0.967	0.828	0.789
1.000	1.014	0.948	1.006	0.995	0.929	1.011	0.936	0.989	0.970	0.956	0.817	0.811
2.000	1.018	0.985	1.026	1.020	0.949	1.012	0.956	1.008	0.987	0.996	0.870	0.876
3.000	1.003	0.988	1.052	1.013	0.949	0.988	0.949	0.992	0.968	1.021	0.868	0.896
4.000	1.041	1.032	1.052	1.001	0.915	0.986	0.920	1.011	0.956	0.997	0.864	0.918
6.000	0.989	0.998	1.030	0.995	0.840	0.933	0.834	0.956	0.903	0.969	0.865	0.888
8.000	0.973	0.967	0.988	0.967	0.778	0.874	0.815	0.890	0.863	0.921	0.850	0.876
10.000	0.963	0.933	0.931	0.969	0.718	0.827	0.771	0.821	0.826	0.911	0.806	0.844

Table 8. Organ equivalent dose conversion coefficients in Sv Gy^{-1} of skin and stomach.

Energy	AP		PA		LLAT		RLAT		ROT		ISO	
(MeV)	Rex	Regina	Rex	Regina	Rex	Regina	Rex	Regina	Rex	Regina	Rex	Regina
						Skin						
0.010	0.230	0.257	0.226	0.252	0.120	0.131	0.119	0.131	0.188	0.208	0.154	0.172
0.015	0.387	0.410	0.373	0.393	0.207	0.214	0.203	0.215	0.324	0.342	0.287	0.303
0.020	0.503	0.526	0.484	0.504	0.277	0.285	0.269	0.287	0.424	0.443	0.386	0.403
0.030	0.694	0.728	0.680	0.715	0.403	0.421	0.392	0.423	0.590	0.620	0.544	0.566
0.040	0.867	0.905	0.860	0.902	0.518	0.539	0.506	0.543	0.742	0.778	0.675	0.703
0.050	1.005	1.044	0.998	1.041	0.613	0.633	0.600	0.636	0.863	0.897	0.782	0.807
0.060	1.093	1.129	1.082	1.127	0.675	0.692	0.662	0.698	0.940	0.974	0.848	0.872
0.070	1.096	1.125	1.089	1.124	0.686	0.702	0.675	0.707	0.949	0.976	0.855	0.877
0.080	1.150	1.174	1.137	1.169	0.724	0.738	0.714	0.744	0.994	1.019	0.895	0.915
0.100	1.136	1.161	1.122	1.151	0.732	0.746	0.720	0.749	0.987	1.011	0.892	0.910
0.150	1.089	1.099	1.069	1.090	0.724	0.734	0.713	0.737	0.949	0.968	0.866	0.876
0.200	1.055	1.069	1.034	1.052	0.717	0.728	0.709	0.732	0.925	0.945	0.848	0.861
0.300	1.017	1.025	0.996	1.011	0.716	0.727	0.709	0.731	0.900	0.914	0.834	0.840
0.400	0.987	0.997	0.970	0.980	0.714	0.724	0.708	0.728	0.885	0.896	0.821	0.824
0.500	0.963	0.969	0.943	0.953	0.716	0.720	0.709	0.726	0.869	0.881	0.809	0.815
0.600	0.944	0.942	0.923	0.925	0.709	0.712	0.704	0.720	0.852	0.861	0.797	0.799
0.800	0.894	0.888	0.879	0.872	0.699	0.697	0.691	0.698	0.822	0.818	0.774	0.768
1.000	0.851	0.832	0.832	0.817	0.679	0.674	0.673	0.678	0.789	0.781	0.747	0.737
2.000	0.702	0.682	0.683	0.670	0.615	0.608	0.614	0.611	0.671	0.658	0.652	0.637
3.000	0.633	0.616	0.625	0.609	0.586	0.581	0.585	0.582	0.620	0.612	0.605	0.596
4.000	0.593	0.580	0.587	0.578	0.571	0.566	0.569	0.567	0.588	0.581	0.579	0.566
6.000	0.544	0.533	0.548	0.540	0.552	0.548	0.551	0.548	0.552	0.545	0.547	0.535
8.000	0.515	0.505	0.520	0.511	0.536	0.534	0.536	0.534	0.529	0.523	0.524	0.512
10.000	0.493	0.481	0.498	0.490	0.526	0.522	0.526	0.522	0.513	0.503	0.504	0.498
						Stomach						
0.010	0.000	0.000	0.000	0.000	0.000	0.000	0.000	0.000	0.000	0.000	0.000	0.000
0.015	0.002	0.007	0.000	0.000	0.000	0.004	0.000	0.000	0.001	0.003	0.000	0.001
0.020	0.043	0.079	0.001	0.003	0.015	0.049	0.000	0.000	0.014	0.031	0.009	0.019
0.030	0.345	0.443	0.040	0.097	0.194	0.340	0.009	0.023	0.140	0.214	0.104	0.155
0.040	0.785	0.897	0.190	0.332	0.509	0.718	0.064	0.096	0.369	0.483	0.283	0.361
0.050	1.170	1.252	0.390	0.579	0.801	1.023	0.149	0.200	0.613	0.745	0.482	0.558
0.060	1.395	1.486	0.585	0.767	0.986	1.189	0.229	0.276	0.772	0.914	0.603	0.693
0.070	1.445	1.516	0.670	0.844	1.037	1.232	0.270	0.316	0.835	0.948	0.670	0.728
0.080	1.511	1.556	0.743	0.917	1.102	1.282	0.307	0.357	0.903	1.006	0.702	0.767
0.100	1.461	1.484	0.774	0.922	1.084	1.239	0.329	0.379	0.890	0.993	0.706	0.758
0.150	1.281	1.312	0.735	0.855	0.996	1.126	0.338	0.385	0.821	0.901	0.661	0.703
0.200	1.186	1.214	0.715	0.823	0.955	1.069	0.350	0.399	0.784	0.855	0.639	0.675
0.300	1.087	1.151	0.693	0.800	0.921	1.011	0.375	0.426	0.761	0.834	0.607	0.663
0.400	1.059	1.089	0.699	0.799	0.899	1.017	0.409	0.460	0.748	0.816	0.623	0.667
0.500	1.025	1.072	0.717	0.779	0.912	0.994	0.437	0.488	0.747	0.821	0.621	0.674
0.600	1.020	1.066	0.733	0.823	0.913	1.004	0.457	0.515	0.749	0.827	0.632	0.675
0.800	1.001	1.031	0.731	0.812	0.914	0.992	0.507	0.558	0.763	0.825	0.664	0.715
1.000	0.994	1.034	0.761	0.836	0.909	0.990	0.541	0.590	0.771	0.856	0.668	0.707
2.000	0.988	1.020	0.836	0.876	0.953	1.015	0.657	0.704	0.824	0.871	0.738	0.793
3.000	1.008	1.028	0.855	0.905	0.968	1.028	0.724	0.752	0.850	0.910	0.787	0.834
4.000	0.998	1.003	0.877	0.925	0.981	1.029	0.756	0.785	0.897	0.904	0.819	0.843
6.000	0.990	1.017	0.902	0.940	0.984	1.019	0.791	0.826	0.902	0.959	0.822	0.889
8.000	1.009	1.018	0.907	0.945	0.995	1.008	0.815	0.842	0.918	0.936	0.874	0.884
10.000	0.994	0.992	0.910	0.948	0.982	0.987	0.817	0.860	0.898	0.931	0.860	0.868

Table 9. Organ equivalent dose conversion coefficients in Sv Gy^{-1} of thyroid and remainder tissues (see table 2 or ICRP (2006)).

Energy	AP		PA		LLAT		RLAT		ROT		ISO	
(MeV)	Rex	Regina	Rex	Regina	Rex	Regina	Rex	Regina	Rex	Regina	Rex	Regina
						Thyroid						
0.010	0.001	0.002	0.000	0.000	0.000	0.000	0.000	0.000	0.000	0.000	0.000	0.000
0.015	0.065	0.093	0.000	0.000	0.004	0.000	0.006	0.000	0.020	0.024	0.010	0.012
0.020	0.303	0.369	0.000	0.000	0.036	0.002	0.051	0.010	0.105	0.118	0.063	0.068
0.030	0.870	0.953	0.027	0.038	0.182	0.032	0.229	0.092	0.354	0.375	0.235	0.246
0.040	1.300	1.361	0.175	0.202	0.343	0.110	0.405	0.220	0.595	0.628	0.408	0.429
0.050	1.607	1.649	0.351	0.446	0.474	0.207	0.553	0.376	0.813	0.832	0.588	0.614
0.060	1.758	1.855	0.512	0.605	0.584	0.293	0.635	0.457	0.940	0.966	0.685	0.726
0.070	1.731	1.808	0.589	0.711	0.607	0.339	0.686	0.506	0.937	1.008	0.686	0.771
0.080	1.788	1.853	0.689	0.759	0.660	0.376	0.715	0.530	1.038	1.034	0.766	0.837
0.100	1.714	1.719	0.740	0.783	0.659	0.385	0.720	0.552	1.040	1.060	0.768	0.814
0.150	1.551	1.547	0.708	0.773	0.637	0.372	0.708	0.536	0.962	0.976	0.744	0.755
0.200	1.460	1.452	0.715	0.747	0.628	0.380	0.703	0.536	0.938	0.913	0.698	0.730
0.300	1.334	1.359	0.724	0.737	0.613	0.382	0.702	0.526	0.912	0.905	0.711	0.709
0.400	1.322	1.301	0.732	0.738	0.646	0.415	0.712	0.545	0.888	0.909	0.705	0.723
0.500	1.223	1.253	0.743	0.768	0.647	0.438	0.717	0.560	0.877	0.855	0.738	0.711
0.600	1.194	1.267	0.757	0.769	0.670	0.442	0.720	0.590	0.879	0.894	0.690	0.740
0.800	1.186	1.216	0.779	0.763	0.682	0.493	0.747	0.624	0.893	0.895	0.744	0.777
1.000	1.182	1.180	0.781	0.809	0.720	0.527	0.772	0.649	0.885	0.913	0.818	0.723
2.000	1.128	1.151	0.874	0.856	0.805	0.656	0.838	0.749	0.945	0.951	0.781	0.842
3.000	1.090	1.137	0.909	0.883	0.821	0.709	0.863	0.807	0.938	0.945	0.845	0.877
4.000	1.095	1.101	0.920	0.911	0.869	0.740	0.896	0.843	0.947	0.966	0.861	0.946
6.000	1.027	1.045	0.958	0.949	0.881	0.818	0.915	0.888	0.967	0.985	0.847	0.925
8.000	0.948	0.860	0.919	0.941	0.898	0.836	0.919	0.901	0.916	0.924	0.873	0.879
10.000	0.799	0.733	0.911	0.951	0.889	0.833	0.910	0.895	0.899	0.881	0.859	0.885
						Remainder tissues						
0.010	0.001	0.000	0.000	0.000	0.001	0.000	0.001	0.000	0.001	0.000	0.001	0.000
0.015	0.015	0.011	0.004	0.004	0.006	0.004	0.006	0.004	0.008	0.006	0.006	0.004
0.020	0.057	0.055	0.019	0.021	0.019	0.020	0.018	0.016	0.028	0.027	0.022	0.020
0.030	0.244	0.284	0.136	0.161	0.091	0.118	0.083	0.093	0.143	0.167	0.106	0.118
0.040	0.541	0.627	0.365	0.428	0.232	0.294	0.216	0.239	0.353	0.404	0.266	0.297
0.050	0.840	0.950	0.619	0.696	0.392	0.468	0.364	0.394	0.576	0.647	0.435	0.484
0.060	1.048	1.150	0.814	0.906	0.512	0.603	0.482	0.514	0.747	0.818	0.576	0.622
0.070	1.120	1.215	0.895	0.982	0.566	0.654	0.532	0.569	0.807	0.885	0.638	0.668
0.080	1.197	1.292	0.982	1.056	0.619	0.704	0.583	0.619	0.885	0.947	0.689	0.728
0.100	1.181	1.266	0.991	1.062	0.635	0.717	0.606	0.633	0.892	0.952	0.703	0.728
0.150	1.079	1.154	0.932	0.989	0.619	0.692	0.592	0.620	0.840	0.891	0.668	0.691
0.200	1.017	1.088	0.893	0.947	0.610	0.681	0.581	0.614	0.809	0.856	0.654	0.673
0.300	0.971	1.027	0.866	0.919	0.609	0.681	0.586	0.622	0.791	0.835	0.636	0.659
0.400	0.937	0.994	0.853	0.904	0.624	0.693	0.600	0.637	0.785	0.826	0.647	0.663
0.500	0.930	0.980	0.849	0.891	0.636	0.709	0.612	0.653	0.786	0.824	0.656	0.673
0.600	0.922	0.970	0.848	0.885	0.650	0.720	0.625	0.665	0.792	0.833	0.666	0.684
0.800	0.917	0.963	0.858	0.899	0.676	0.746	0.650	0.695	0.798	0.838	0.678	0.705
1.000	0.924	0.963	0.867	0.904	0.701	0.760	0.677	0.714	0.815	0.853	0.697	0.717
2.000	0.940	0.978	0.900	0.932	0.777	0.837	0.756	0.791	0.864	0.892	0.773	0.791
3.000	0.955	0.986	0.923	0.952	0.816	0.870	0.801	0.839	0.891	0.925	0.804	0.825
4.000	0.968	0.993	0.932	0.959	0.842	0.884	0.825	0.851	0.901	0.934	0.829	0.858
6.000	0.959	0.993	0.954	0.976	0.869	0.916	0.852	0.881	0.926	0.946	0.854	0.872
8.000	0.950	0.983	0.946	0.963	0.873	0.919	0.859	0.891	0.919	0.944	0.855	0.886
10.000	0.925	0.960	0.945	0.961	0.876	0.922	0.857	0.896	0.918	0.935	0.867	0.881

Table 10. Organ equivalent dose conversion coefficients in Sv Gy^{-1} of urinary bladder and eye lenses.

Energy	AP		PA		LLAT		RLAT		ROT		ISO	
(MeV)	Rex	Regina	Rex	Regina	Rex	Regina	Rex	Regina	Rex	Regina	Rex	Regina
						Urinary bladder						
0.010	0.000	0.002	0.000	0.000	0.000	0.000	0.000	0.000	0.000	0.000	0.000	0.000
0.015	0.003	0.072	0.000	0.000	0.000	0.000	0.000	0.000	0.001	0.018	0.000	0.011
0.020	0.053	0.229	0.001	0.000	0.000	0.000	0.000	0.000	0.012	0.067	0.007	0.049
0.030	0.357	0.661	0.060	0.039	0.014	0.020	0.008	0.019	0.116	0.224	0.081	0.172
0.040	0.772	1.098	0.248	0.182	0.076	0.094	0.057	0.091	0.312	0.426	0.226	0.350
0.050	1.142	1.468	0.495	0.372	0.175	0.186	0.143	0.193	0.537	0.618	0.374	0.506
0.060	1.400	1.687	0.689	0.521	0.275	0.281	0.235	0.273	0.721	0.756	0.510	0.627
0.070	1.428	1.692	0.798	0.602	0.337	0.334	0.288	0.332	0.775	0.800	0.571	0.661
0.080	1.534	1.798	0.882	0.706	0.380	0.372	0.330	0.368	0.858	0.892	0.627	0.710
0.100	1.541	1.706	0.905	0.728	0.413	0.408	0.378	0.409	0.868	0.901	0.636	0.730
0.150	1.353	1.523	0.865	0.700	0.424	0.417	0.386	0.414	0.804	0.827	0.614	0.675
0.200	1.263	1.399	0.857	0.678	0.434	0.432	0.391	0.432	0.781	0.780	0.592	0.648
0.300	1.132	1.283	0.797	0.668	0.462	0.449	0.412	0.447	0.731	0.763	0.592	0.647
0.400	1.130	1.227	0.806	0.679	0.485	0.485	0.439	0.485	0.747	0.774	0.598	0.634
0.500	1.111	1.202	0.782	0.692	0.515	0.523	0.482	0.510	0.756	0.763	0.603	0.678
0.600	1.074	1.171	0.805	0.721	0.544	0.546	0.503	0.536	0.745	0.772	0.595	0.659
0.800	1.052	1.112	0.818	0.773	0.580	0.561	0.534	0.550	0.763	0.765	0.618	0.689
1.000	1.052	1.096	0.823	0.746	0.586	0.609	0.573	0.598	0.766	0.784	0.663	0.703
2.000	1.020	1.096	0.851	0.829	0.697	0.713	0.693	0.697	0.808	0.824	0.727	0.780
3.000	1.007	1.091	0.911	0.848	0.768	0.792	0.763	0.755	0.871	0.889	0.782	0.780
4.000	1.056	1.065	0.890	0.883	0.785	0.790	0.768	0.808	0.896	0.897	0.804	0.851
6.000	1.050	0.999	0.910	0.916	0.834	0.823	0.813	0.827	0.908	0.895	0.830	0.849
8.000	1.036	0.899	0.933	0.934	0.833	0.859	0.813	0.839	0.919	0.922	0.843	0.826
10.000	1.022	0.876	0.940	0.907	0.859	0.868	0.850	0.854	0.908	0.853	0.855	0.831
						Eye lenses						
0.010	0.293	0.047	0.000	0.000	0.002	0.003	0.000	0.004	0.079	0.015	0.044	0.015
0.015	0.725	0.400	0.000	0.000	0.085	0.102	0.054	0.102	0.239	0.160	0.159	0.116
0.020	0.948	0.739	0.000	0.000	0.245	0.281	0.190	0.270	0.368	0.342	0.321	0.247
0.030	1.219	1.158	0.001	0.007	0.502	0.535	0.407	0.474	0.562	0.593	0.440	0.522
0.040	1.362	1.277	0.021	0.034	0.677	0.684	0.617	0.668	0.733	0.782	0.626	0.466
0.050	1.558	1.414	0.035	0.079	0.915	0.905	0.779	0.872	0.856	0.826	0.605	0.704
0.060	1.479	1.531	0.087	0.120	0.974	1.030	0.878	1.031	0.990	1.017	0.634	0.907
0.070	1.539	1.532	0.210	0.161	0.950	1.086	0.919	0.986	0.851	0.941	0.795	0.920
0.080	1.668	1.548	0.142	0.203	1.177	1.034	1.006	1.053	1.074	0.996	0.771	0.969
0.100	1.756	1.467	0.162	0.227	1.141	1.124	1.083	1.050	1.006	0.985	0.897	0.847
0.150	1.625	1.539	0.228	0.212	1.079	1.159	0.991	1.037	0.988	1.007	0.918	0.907
0.200	1.428	1.327	0.231	0.336	1.123	1.097	0.950	1.025	1.004	0.927	1.019	0.980
0.300	1.243	1.251	0.260	0.354	1.018	1.091	0.931	0.925	0.979	0.998	0.734	0.957
0.400	1.234	1.297	0.320	0.367	1.029	1.016	1.004	1.022	0.998	0.968	1.089	0.661
0.500	1.195	1.172	0.353	0.493	1.079	1.029	0.979	1.020	0.904	0.948	1.092	0.797
0.600	1.202	1.228	0.436	0.475	1.004	1.024	1.025	1.010	0.975	0.924	0.818	0.970
0.800	1.148	1.203	0.361	0.491	0.976	1.014	0.923	1.030	1.022	1.078	0.946	0.975
1.000	1.153	1.078	0.539	0.520	1.016	1.003	1.054	1.001	0.959	1.022	0.997	0.729
2.000	0.787	1.063	0.573	0.675	1.044	1.055	0.986	0.989	0.864	0.924	0.985	0.925
3.000	0.550	0.872	0.665	0.702	0.937	1.000	0.976	0.991	0.787	0.903	0.946	1.037
4.000	0.406	0.691	0.768	0.828	0.934	0.971	0.905	0.932	0.697	0.881	0.620	0.909
6.000	0.262	0.446	0.756	0.819	0.834	0.842	0.890	0.861	0.706	0.739	1.018	0.446
8.000	0.159	0.338	0.804	0.843	0.771	0.766	0.768	0.765	0.649	0.661	0.630	0.791
10.000	0.155	0.286	0.816	0.900	0.696	0.689	0.769	0.710	0.637	0.645	0.667	0.719

Table 11. The effective dose conversion coefficients in Sv Gy^{-1} resulting from Rex and Regina using either the definition of ICRP Publication 60 (ICRP 1991) or of the ICRP draft recommendations (ICRP 2006).

Energy	AP		PA		LLAT		RLAT		ROT		ISO	
(MeV)	Rex	Regina	Rex	Regina	Rex	Regina	Rex	Regina	Rex	Regina	Rex	Regina
0.010	0.006	0.010	0.002	0.002	0.002	0.003	0.002	0.002	0.003	0.005	0.003	0.004
0.015	0.036	0.051	0.004	0.005	0.008	0.015	0.007	0.014	0.015	0.022	0.013	0.019
0.020	0.114	0.135	0.013	0.014	0.023	0.042	0.020	0.037	0.048	0.060	0.038	0.049
0.030	0.413	0.426	0.120	0.114	0.110	0.148	0.084	0.119	0.198	0.212	0.154	0.169
0.040	0.784	0.780	0.360	0.338	0.254	0.306	0.201	0.248	0.423	0.434	0.330	0.343
0.050	1.100	1.086	0.619	0.584	0.401	0.462	0.329	0.383	0.650	0.657	0.507	0.519
0.060	1.308	1.287	0.816	0.773	0.510	0.575	0.429	0.486	0.810	0.811	0.637	0.645
0.070	1.351	1.330	0.906	0.857	0.557	0.618	0.473	0.527	0.866	0.867	0.683	0.690
0.080	1.423	1.401	0.987	0.935	0.601	0.665	0.519	0.573	0.926	0.930	0.741	0.747
0.100	1.384	1.363	0.997	0.951	0.611	0.674	0.534	0.587	0.922	0.929	0.745	0.754
0.150	1.240	1.232	0.926	0.894	0.591	0.647	0.524	0.573	0.859	0.868	0.693	0.708
0.200	1.164	1.159	0.888	0.861	0.580	0.634	0.523	0.570	0.823	0.836	0.675	0.688
0.300	1.090	1.090	0.861	0.841	0.586	0.635	0.534	0.577	0.801	0.815	0.661	0.676
0.400	1.057	1.055	0.852	0.836	0.603	0.649	0.553	0.592	0.797	0.808	0.660	0.677
0.500	1.035	1.033	0.853	0.836	0.619	0.662	0.574	0.610	0.794	0.807	0.669	0.686
0.600	1.024	1.024	0.857	0.842	0.632	0.674	0.588	0.624	0.802	0.813	0.681	0.699
0.800	1.005	1.009	0.859	0.850	0.659	0.697	0.619	0.651	0.814	0.824	0.704	0.714
1.000	1.000	1.003	0.875	0.865	0.683	0.717	0.647	0.676	0.822	0.834	0.714	0.727
2.000	0.999	0.994	0.905	0.901	0.765	0.791	0.739	0.760	0.867	0.874	0.785	0.791
3.000	0.998	0.985	0.932	0.925	0.812	0.829	0.785	0.799	0.895	0.896	0.818	0.821
4.000	0.989	0.974	0.939	0.936	0.835	0.848	0.812	0.822	0.906	0.907	0.842	0.837
6.000	0.970	0.947	0.959	0.952	0.859	0.863	0.842	0.843	0.920	0.913	0.842	0.842
8.000	0.942	0.918	0.961	0.955	0.864	0.863	0.849	0.845	0.906	0.899	0.858	0.852
10.000	0.909	0.884	0.958	0.952	0.866	0.860	0.855	0.846	0.903	0.891	0.850	0.841

from the previous ones also in other aspects such as transport code, photon cross sections and organ compositions (media). We verified that all of these latter improvements affect the dose conversion coefficients below about 40 keV, with the highest changes being at most 20% below 15 keV. The pursuit of secondary electrons instead of using the kerma approximation also influences the dose conversion coefficients of surface organs like skin and breast tissue for energies higher than about 400 keV. For these energies, not all electrons that are created in a thin organ are absorbed in this organ; thus, the resulting dose conversion coefficients are reduced compared to those computed with kerma approximation.

Hence, most of the differences in the organ dose conversion coefficients between this study and ICRP 74 are due to the different anatomy of the employed models, confirming earlier findings by other authors (Jones 1997, Chao *et al* 2001, Ferrari and Gualdrini 2005, Kramer *et al* 2005), who used their own voxel models for a comparison with ICRP 74. A very comprehensive survey in this context has been performed by Zankl *et al* (2002), who confronted the dose conversion coefficients of seven voxel models of different stature with their respective results (Zankl *et al* 1997) for the two mathematical reference models Adam and Eva (Kramer *et al* 1982). Thus, the intrinsic shortcomings in the anatomy of the mathematical models could be inferred. For instance, many of the detected differences in the dose conversion coefficients can be explained by the un-natural shape of the human abdomen of the mathematical models, which is composed of an extended ellipsoid to include the arms. This shape is completely different to real anatomy, where the abdomen is rather rectangular and the arms are not located centrally at each side, but rather towards the back.

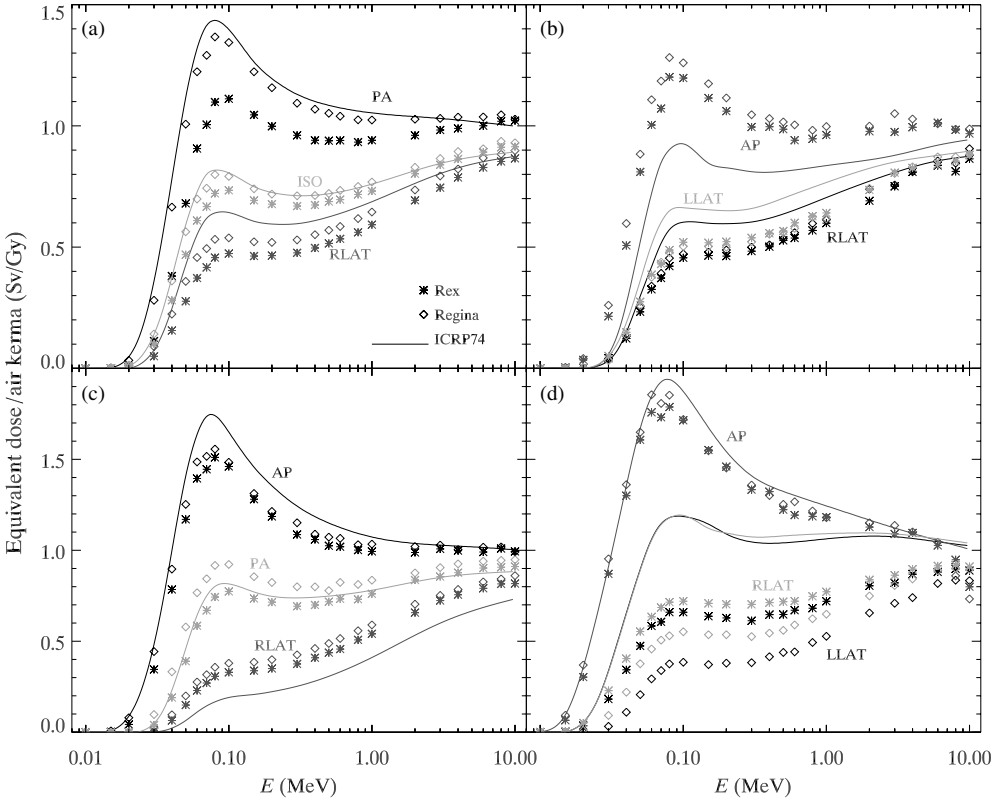

Figure 3. Comparison of dose conversion coefficients for lungs (a), oesophagus (b), stomach (c) and thyroid (d) of Rex, Regina and the reference values of ICRP 74 (1996) for the indicated geometries. The 2σ uncertainty range is always smaller than the symbol size, in most cases even much less.

As a result of this particular difference in mathematical and voxel models, higher dose conversion coefficients for right-side lateral exposure are observed in Rex and Regina, in particular for the colon, pancreas and the stomach (figure 3). Lower dose conversion coefficients in Rex and Regina are obtained for active bone marrow and thyroid. Furthermore, lungs and thymus are apparently better shielded by the rib cage of Rex and Regina, and thus their dose values are smaller than in the mathematical models. As found by Lee *et al* (2006) the wrong location of the arms in the stylized models also contributes for lateral exposures to the overestimation of the lung dose by mathematical models.

Except for the pancreas, the same trends are apparent for left-side lateral irradiation. In this case, the dose conversion coefficients for the pancreas are similar in mathematical and voxel phantoms. Higher conversion coefficients emerge for the liver, which is less shielded in Rex and Regina from left-lateral irradiation compared to the mathematical models.

In AP geometry stomach and thymus receive less dose in Rex and Regina, but the dose conversion coefficients of active bone marrow and, especially, oesophagus are underestimated by ICRP (1996) (figures 3(b), (c)). The latter is located extremely posterior in the mathematical models Adam and Eva, which explains its rather large conversion coefficient in the PA direction.

Higher dose conversion coefficients are also obtained for thymus and thyroid of Rex and Regina in PA geometry. These organs are shielded more by the spine in the mathematical

models. Still, lower conversion coefficients are obtained in Rex and Regina for active bone marrow as well as for small and large intestine, kidneys and pancreas. This indicates that the distance of intestine, kidneys and pancreas to the back of the body is underestimated by the mathematical models and/or the organs are located more anterior.

4.2. Comparison of the dose conversion coefficients of Rex and Regina

The smaller stature of the female model leads, as expected, to higher dose conversion coefficients in Regina compared to Rex in almost all organs and all examined geometries (cf figure 3). A standard exception is the lungs in AP, where the higher shielding by the female breast yields lower conversion coefficients compared to the male model.

In absolute values, the organ dose conversion coefficients show their largest deviations at photon energies around 40–80 keV. For unidirectional irradiation, i.e., AP, PA, LLAT and RLAT, the coefficients can be up to 0.2 Sv Gy^{-1} higher in Regina. The more isotropic the irradiation, the smaller the differences, such that in ROT and ISO geometry the largest deviation is 0.1 Sv Gy^{-1}. The reason certainly is that the exact location of an organ is less important for rotating and isotropic sources, because even near-surface organs are not always directly irradiated.

Considering relative differences, these are in the same energy range (40–80 keV) at most about 50% for unidirectional irradiations. In most cases, the deviations grow strongly towards lower energies. With decreasing photon energy, the depth of an organ within the human body becomes an increasingly crucial parameter strongly influencing the usually small organ dose conversion coefficients. This can lead to high relative differences between Rex and Regina of 100% or more for conversion coefficients below about 20–30 keV photon energy.

In summary, the largest discrepancies between Regina and Rex in AP direction are found for colon, liver, urinary bladder, pancreas, spleen, kidneys and adrenals. It is however worth noting that particularly the positions of organs of the alimentary tract strongly depend on the individual person's position, and the composition and time of his/her last meal. Similarly, kidneys and adrenals show strong variances between different persons, which is somehow reflected by the conversion-coefficient differences of Regina and Rex.

For PA geometry, the dose conversion coefficients for lungs, stomach and thymus are noticeably higher in Regina (figure 3(c)). Interestingly, the conversion coefficient to the adrenals is smaller in the female model, because they are more shielded by the kidneys than in the male model. This again just displays the effect of individual differences.

In left-side lateral exposure direction colon, stomach and spleen have higher dose conversion coefficients, while in right-side lateral geometry only the conversion coefficient to the adrenals is higher. The dose conversion coefficient of the thyroid is considerably lower in Regina for both lateral irradiation geometries, which is even more pronounced for LLAT (figure 3(d)). Apparently, the shoulders are located higher in the female phantom, and her left shoulder is higher than her right one.

For rotational and isotropic sources, the dose conversion coefficients are almost the same for all organs of Regina and Rex (e.g., the lungs, figure 3(a)). Only very small discrepancies are noticeable for liver, pancreas, stomach and spleen in ROT exposure, and urinary bladder in ISO geometry.

4.3. The effective dose conversion coefficients

The organ dose conversion coefficients of the phantoms Rex and Regina have been used to compute the effective dose conversion coefficient. Two different sets of tissue weighting

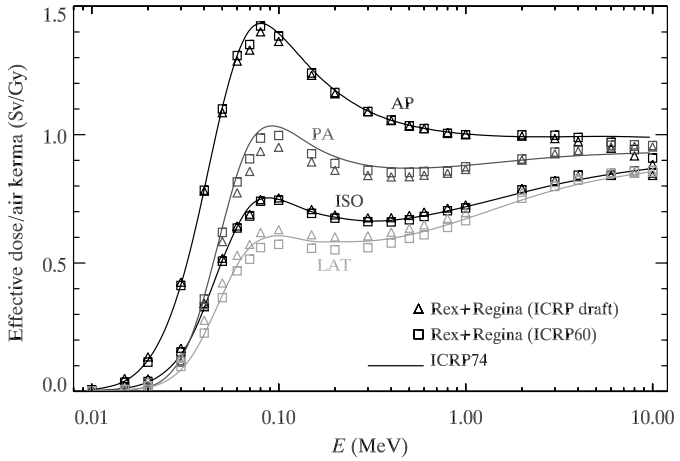

Figure 4. Comparison of effective dose conversion coefficients from ICRP 74 (1996) with values obtained from the phantoms Rex and Regina, using either the definition of ICRP 60 (1991) or of the draft recommendations (ICRP 2006). LAT denotes the mean of RLAT and LLAT.

factors have been applied, the standard one from ICRP Publication 60 (ICRP 1991) and a new one from the ICRP draft recommendations (ICRP 2006) (table 2), which is still under discussion. The organ-specific tissue weighting factors were applied to the arithmetic mean of the organ doses for the male and the female phantom. In both cases, the remainder dose conversion coefficients have been calculated as the arithmetic mean values of the conversion coefficients of the respective remainder organs for Rex and Regina separately, and then the arithmetic mean of these two gender-specific remainder dose conversion coefficients was evaluated. The footnote-3 rule of ICRP 60 has been ignored; this rule increases the weighting factor of a remainder organ in the case it receives a dose higher than any of the organs with a specific tissue weighting factor. The impact of that rule on the effective dose for external exposure is negligible and only introduces inconsistencies which complicate the interpretation of the resulting values (Zankl and Drexler 1995). As the bone surface is not resolved in the voxel models (and neither in the mathematical models), the dose conversion coefficient of spongiosa has been used as a substitute value, as recommended by Eckerman (2006).

Since the effective dose conversion coefficient is a weighted mean over many organs, smaller differences are expected compared to ICRP Publication 74 (ICRP 1996) than for the dose conversion coefficients in individual organs. Indeed, for AP and ISO geometry almost the same effective dose conversion coefficient is obtained with Rex and Regina as in ICRP 74, and it is also independent of whether the definition of ICRP 60 (ICRP 1991) or the ICRP draft (ICRP 2006) is employed (figure 4). The largest differences can be observed for PA and lateral irradiations, although the absolute values still only differ by at most a few hundredths Sv Gy^{-1}. Anyway, in those cases the new weighting factors of the ICRP draft recommendations have the biggest impact. The lower effective dose conversion coefficients for PA are mostly caused by the smaller conversion coefficients of highly weighted organs such as active bone marrow, lung and large intestine in Rex and Regina (see section 4.1). For lateral exposures, the amount by which the dose conversion coefficients in the voxel models for lung, active bone marrow, oesophagus and thyroid are lower slightly exceeds the amount by which the coefficients of colon and stomach are higher, such that a moderately diminished effective dose conversion coefficient is obtained, compared to the ICRP 74 values. Nevertheless, the increased tissue weighting for breast and remainder and the demoting of the

gonads in the ICRP draft recommendations yield an effective dose conversion coefficient for lateral exposures, which is even somewhat higher than that of ICRP Publication 74.

5. Conclusion

A new set of organ equivalent dose conversion coefficients has been presented for external photon exposure in standardized geometries. They are based on voxel models representing the ICRP Reference Male and Female. These models have been developed in close cooperation with the ICRP to become the ICRP standard reference human models. The coefficients have been computed with a user code to EGSnrc (Kawrakow and Rogers 2003), a Monte Carlo transport code comprising contemporary physics.

The determination of the active bone marrow dose has been performed with a modified version of the method described by Zankl *et al* (2002), i.e., applying correction factors to the mean spongiosa doses, but considering the partitioning of active bone marrow to the different bones according to ICRP Publication 89 (ICRP 2002). In the near future bone-specific fluence-to-dose response functions will become available, which are to be multiplied with the particle fluence inside individual bones to yield the respective equivalent dose. Hence, the presented dose values for RBM and bone surface (substituted here by spongiosa) might soon be replaced. Nevertheless, it could be demonstrated that the exact partitioning of the voxels into the different bone components is of minor importance for the resulting red bone marrow dose. Therefore, for external exposure, great changes in the RBM dose conversion coefficients are not expected with the forthcoming fluence-to-dose response functions.

For most organs, the new dose conversion coefficients deviate about 10% from the currently valid reference values of ICRP (1996), which are based on mathematical models. However, for some organs, including many with large contribution to the effective dose, the differences amount to about 30% or even higher for certain geometries. For instance, in RLAT direction the dose conversion coefficients to the lungs at 100 keV are about 30% less than the value of ICRP 74 (1996), while the conversion coefficient of the stomach is in that geometry 50% higher. Overall, we confirm the results found by previous authors, attributing the main differences to the improved anatomy.

The presented dose conversion coefficients do not only differ from the values of ICRP 74, but show as well a noticeable dependence on the sex. The smaller stature of the average female leads in many cases to higher organ dose conversion coefficients, which can amount to 30–50% or more. Nevertheless, conversion coefficients of organs with a rather variant location in the human body do not necessarily show this behaviour, as for instance the adrenals. Some of the discrepancies found between organ dose conversion coefficients of the present female and male phantom are thus not sex-specific, but rather reflect somewhat the variations between different individuals. This is a general feature of voxel models, which are all based on CT or MRI data of single humans. Their individual organ positions are somewhat maintained also in those voxel models, which have been adjusted to comply with ICRP reference values. In any case, since voxel models reproduce the human anatomy better than the mathematical models, the usage of reference voxel models is certainly to be preferred. A quantification of the influence of individual image data could be achieved by comparing the dose conversion coefficients calculated by several ‘reference’ models, where each is obtained from a different patient data set—but with all other parameters influencing the computations kept constant.

The dose conversion coefficients of many highly weighted organs differ considerably between ICRP 74 and the voxel models Rex and Regina. Nevertheless, the effective dose conversion coefficient itself is only mildly altered with the new models, because the variances in individual organ doses are cancelled for the most part. The biggest changes could be

observed for postero-anterior and lateral exposures. However, the direction of those changes depends on the applied definition of the effective dose. With the current definition of ICRP Publication 60 (ICRP 1991), for both cases the effective dose conversion coefficient has slightly subsided compared to ICRP 74. Employing the proposed definition of ICRP draft recommendations (ICRP 2006), the effective dose conversion coefficient for PA decreases further, while for lateral directions a somewhat higher value is obtained for Rex and Regina compared to the ICRP 74 values.

In conclusion, the changes in the effective dose conversion coefficients are small. Hence, the impact of both, the new phantoms and the ICRP draft recommendations, is moderate in radiation-protection circumstances, where the effective dose conversion coefficient from external photon exposures is the crucial quantity.

Acknowledgments

This work has been financially supported by the German Federal Ministry for the Environment, Nature Conservation and Nuclear Safety under contract no. StSch 4417. The contribution of V Taranenko in the comparison of the dose conversion coefficients obtained with EGSnrc and MCNPX is kindly acknowledged.

References

Becker J, Zankl M and Petoussi N 2007 A software tool for modification of human voxel models used for application in radiation protection *Phys. Med. Biol.* at press

Berger M J and Hubbell J H 1987 XCOM: Photon cross sections on a personal computer *NBSIR* 87-3597 (Gaithersburg, MD: National Bureau of Standards (former name of NIST))

Chao T C, Bozkurt A and Xu X G 2001 Conversion coefficients based on the VIP-Man anatomical model and EGS4-VLSI code for external monoenergetic photons from 10 keV to 10 MeV *Health Phys.* **81** 163–83

Cullen D E, Hubbell J H and Kissel L 1997 EPDL97: the evaluated photon data library *Lawrence Livermore National Laboratory Report* UCRL-50400 vol 6, rev 5

Dimbylow P J (ed) 1996 The development of realistic voxel phantoms for electromagnetic field dosimetry *Workshop on Voxel Phantom Development* (Chilton: National Radiological Protection Board) pp 1–7

Eckerman 2006 Private communication

Ferrari P and Gualdrini G 2005 An improved MCNP version of the NORMAN voxel phantom for dosimetry studies *Phys. Med. Biol.* **50** 4299–316

Gibbs S J, Pujol A, Chen T-S, Malcolm A W and James A E 1984 Patient risk from interproximal radiography *Oral Surg. Oral Med. Oral Pathol.* **58** 347–54

Hendricks J S *et al* 2005 MCNPX extensions, version 2.5.0 LA-UR-05-2675 (Los Alamos, NM: LANL)

ICRP 1975 Reference man: anatomical, physiological and metabolic characteristics *ICRP Publication No 23* (Oxford: Pergamon)

ICRP 1991 1990 Recommendations of the International Commission on Radiological Protection *ICRP Publication No 60* (Oxford: Pergamon)

ICRP 1995 Basic anatomical and physiological data for use in radiological protection: the skeleton *ICRP Publication No 70* (Oxford: Pergamon)

ICRP 1996 Conversion coefficients for use in radiological protection against external radiation *ICRP Publication No 74* (Oxford: Pergamon)

ICRP 2002 Basic anatomical and physiological data for use in radiological protection: reference values *ICRP Publication No 89* (Oxford: Pergamon)

ICRP 2006 Draft recommendations of the International Commission of Radiological Protection 02/276/06

ICRU 1984 Stopping powers for electrons and positrons *ICRU Report No 37* (Bethesda MD: International Commission on Radiation Units and Measurements)

ICRU 1992 Photon, electron, proton and neutron interaction data for body tissues *ICRU Report No 46* (Bethesda, MD: International Commission on Radiation Units and Measurements)

Jones D G 1997 A realistic anthropomorphic phantom for calculating organ doses arising from external photon irradiation *Radiat. Prot. Dosim.* **72** 21–9

Kawrakow I and Bielajew A F 1998 On the condensed history technique for electron transport *Nucl. Instrum. Methods* B **142** 253–80

Kawrakow I and Rogers D W O 2003 The EGSnrc code system: Monte Carlo simulation of electron and photon transport *PIRS Report No 701* (Ottawa: National Research Council of Canada (NRCC))

King S D and Spiers F W 1985 Photoelectron enhancement of the absorbed dose from x rays to human bone marrow: experimental and theoretical studies *Br. J. Radiol.* **58** 345–56

Kramer R, Khoury H J and Vieira J W 2005 Comparison between effective doses for voxel-based and stylized exposure models from photon and electron irradiation *Phys. Med. Biol.* **50** 5105–26

Kramer R, Khoury H J, Vieira J W and Lima V J M 2006 MAX06 and FAX06: update of two adult human phantoms for radiation protection dosimetry *Phys. Med. Biol.* **51** 3331–46

Kramer R, Zankl M, Williams G and Drexler G 1982 The calculation of dose from external photon exposures using reference human phantoms and Monte Carlo methods: part I. The male (Adam) and female (Eva) adult mathematical phantoms *GSF-Report S-885* (Neuherberg, Germany: GSF—National Research Center for Environment and Health)

Lee C, Lee C and Lee J-K 2006 On the need to revise the arm structure in stylized anthropomorphic phantoms in lateral photon irradiation geometry *Phys. Med. Biol.* **51** N393–402

Nelson W R, Hirayama H and Rogers D W O 1985 The EGS4 Code System *SLAC Report No 265* (Stanford, CA: Stanford Linear Accelerator Center)

Petoussi-Henss N, Zankl M, Fill U and Regulla D 2002 The GSF family of voxel phantoms *Phys. Med. Biol.* **47** 89–106

Seuntjens J P, Kawrakow I, Borg J, Hobeila F and Rogers D W O 2002 Calculated and measured air-kerma response of ionization chambers in low and medium energy photon beams *Recent Developments in Accurate Radiation Dosimetry: Proc. Int. Workshop* ed J P Seuntjens and P Mobit (Madison, WI: Medical Physics Publishing) pp 69–84

Snyder W S, Ford M R and Warner G G 1978 Estimates of specific absorbed fractions for monoenergetic photon sources uniformly distributed in various organs of a heterogeneous phantom *MIRD Pamphlet No 5 revised* (New York: Society of Nuclear Medicine)

Taranenko V 2005 Private communication

Taranenko V, Zankl M and Schlattl H 2005 Voxel phantom setup in MCNPX *The Monte Carlo Method: Versatility Unbounded in a Dynamic Computing World (Chattanooga, TN)* (La Grange Park, IL: American Nuclear Society) on CDROM

Ulanovsky A, Wieser A, Zankl M and Jacob P 2005 Photon dose conversion coefficients for the human teeth in standard irradiation geometries *Health Phys.* **89** 645–59

Xu X G, Chao T C and Bozkurt A 2000 VIP-MAN: an image-based whole-body adult male model constructed from color photographs of the Visible Human Project for multi-particle Monte Carlo calculations *Health Phys.* **78** 476–86

Zankl M, Becker J, Fill U, Petoussi-Henß N and Eckerman K F 2005 GSF male and female adult voxel models representing ICRP Reference Man—the present status *The Monte Carlo Method: Versatility Unbounded in a Dynamic Computing World (Chattanooga, TN)* (La Grange Park, IL: American Nuclear Society) on CDROM

Zankl M and Drexler G 1995 An analysis of the equivalent dose calculation for the remainder tissues *Health Phys.* **69** 346–55

Zankl M, Eckerman K F and Bolch W E 2007 Adult male and female voxel-based models representing the ICRP Reference Man—the skeleton *Radiat. Prot. Dosim.* submitted

Zankl M, Fill U, Petoussi-Henss N and Regulla D 2002 Organ dose conversion coefficients for external photon irradiation of male and female voxel models *Phys. Med. Biol.* **47** 2367–85

Zankl M, Petoussi-Henss N, Drexler G and Saito K 1997 The calculation of dose from external photon exposures using reference human phantoms and Monte Carlo methods. Part VII: organ doses due to parallel and environmental exposure geometries *GSF-Report No 8/97* (Neuherberg, Germany: GSF—Forschungszentrum für Umwelt und Gesundheit)

Zankl M, Veit R, Williams G, Schneider K, Fendel H, Petoussi N and Drexler G 1988 The construction of computer tomographic phantoms and their application in radiology and radiation protection *Radiat. Environ. Biophys.* **27** 153–64

Zankl M and Wittmann A 2001 The adult male voxel model 'Golem' segmented from whole body CT patient data *Radiat. Environ. Biophys.* **40** 153–62

Zubal I G, Harrell C R, Smith E O, Rattner Z, Gindi G and Hoffer P B 1994 Computerized three-dimensional segmented human anatomy *Med. Phys.* **21** 299–302